MSUCP-31
June 1980

TRIMMING OF THE MAGNETIC FIELD FOR THE K-500 CYCLOTRON AT MSU

G. Bellomo, F.G. Resmini

Cyclotron Laboratory

Michigan State University, East Lansing, MI 48824

Abstract

The expected final characteristics of the magnetic field of the K-500 cyclotron at MSU are presented, together with the procedures used to properly shape and trim the field. The equilibrium orbits properties of a number of representative ions are also given and discussed in detail.

I. Introduction

Following an extensive magnetic field mapping of the three-sector K-500 cyclotron under construction at MSU,[1] and whose results are reported in (2), it appeared that various field corrections were necessary in order to achieve the desired properties of the cyclotron in terms of axial focusing and isochronism, while keeping the trim-coil power within reasonably low limits. A number of alterations of the iron configuration were also needed for construction reasons, as will be seen in the following.

This paper describes the corrections to the pole tip geometry which were decided and their effects on the field. Upon this basis we then analyze the expected cyclotron performance in terms of the equilibrium orbit properties for a number of representative ions, and the overall trim coils requirements throughout the operating range of the machine.

2. The uncorrected pole tip geometry

For the present purposes it is useful to recall the main features of the coils and pole tip geometry.

A perspective view of a hill and a valley for the uncorrected geometry is given in Fig. 1, while their profiles relative to the median plane are sketched in Fig. 2. The pole radius is 25.75", but the iron structure, as shown in Fig. 1, continues as a part of the inner tank wall from 26" to 28" radius, both for the hill and the valley. There is a .25" gap between the two structures. The upper part of the hill

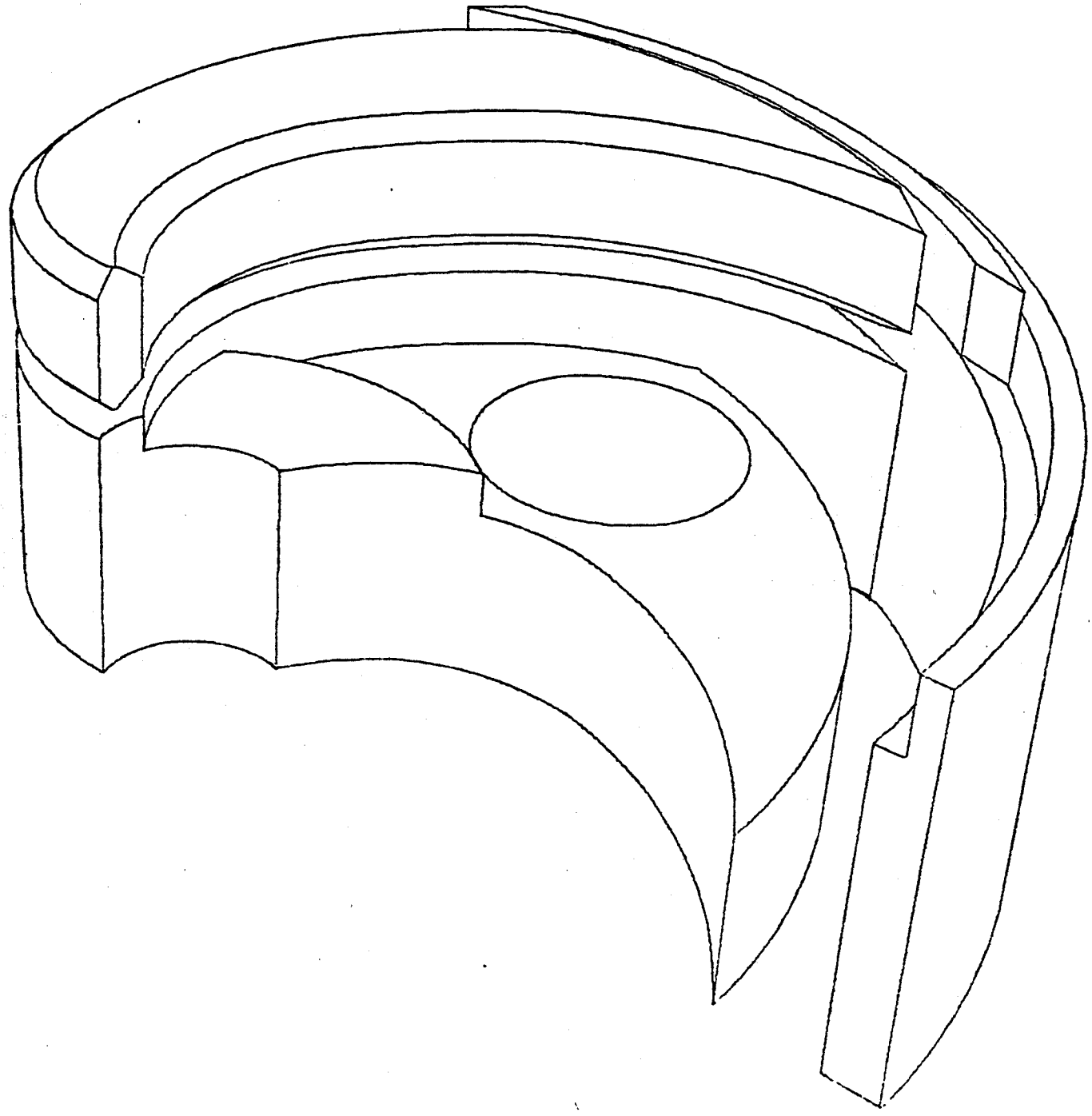

FIG. 1. Perspective view of a sector for the K-500 pole tip geometry.

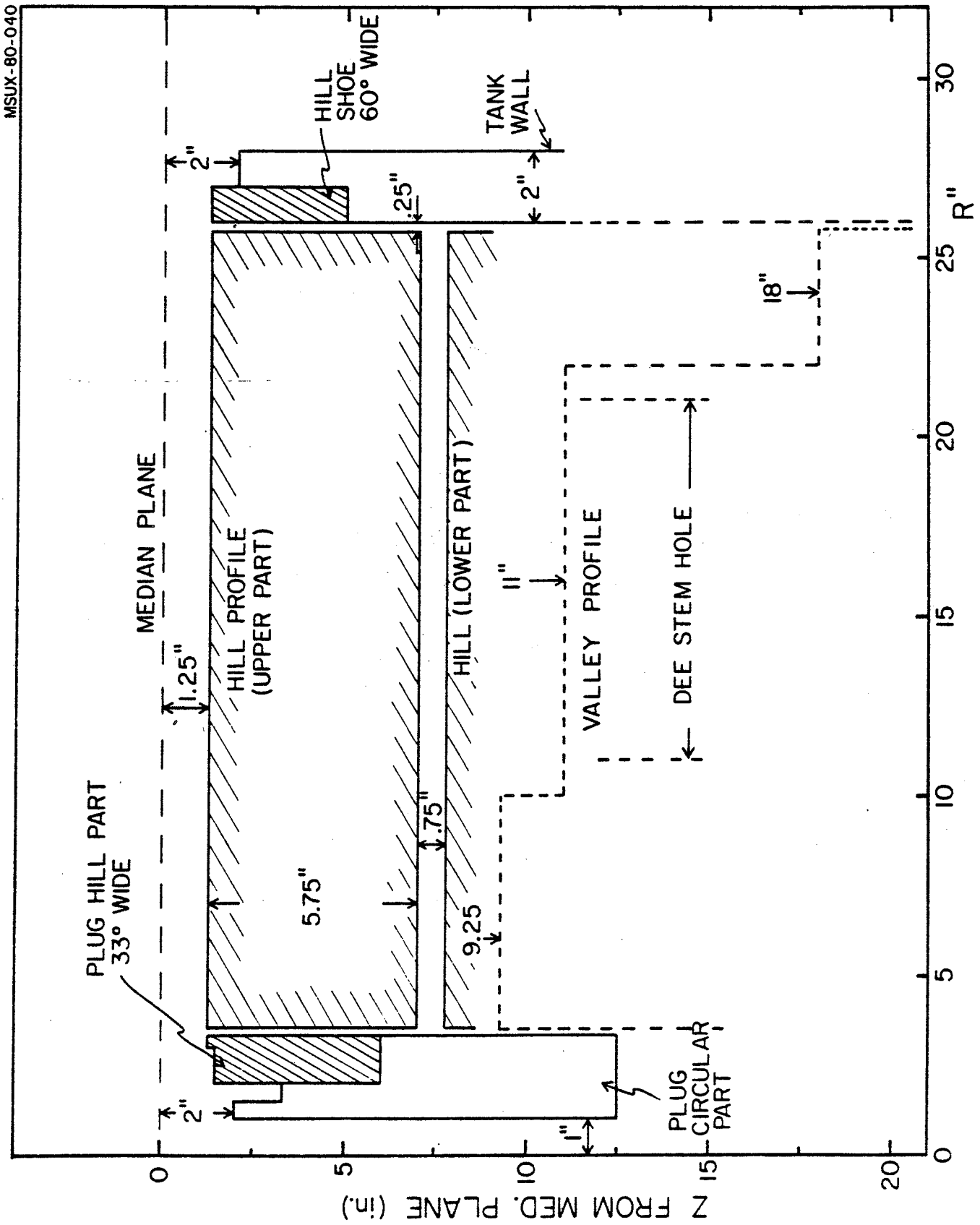

FIG. 2. Radial hill and valley profile of the pole tip geometry.

is 5.75" thick, and it is the one around which the trim coils will be wound. The gap in the hill region is uniformly 2.5", the spiral constant 1/13 rad/inch. The azimuthal hill width starts from 33° at 3.5" radius and reaches 46° at 10", being thereafter essentially constant up to 25.75". The hill shoe inserted in the tank wall is instead 60° wide as noted in Fig. 2.

All essential features of the valleys are represented in self-explanatory way in Fig. 2.

The plug, inserted into the 7.0" diameter central hole, provides a 2" diameter hole for the ion source, and compensates the field. It consists, as shown in Fig. 2, of a cylindrical part and a hill part, more details being given in (2). The coils are split into two independently excited parts, the smaller being the one closer to the median plane. Their currents will be indicated by I_α and I_β respectively, with maximum values around 800 A. The coils dimensions and their air-core fields are shown in Fig. 3.

We write the total average field as a function of radius, as:

$$\overline{B}(r, I_\alpha, I_\beta) = \overline{B}_{iron}(r, I_\alpha, I_\beta) + B_{coils}(r, I_\alpha, I_\beta)$$

therefore splitting it into an iron and a coil produced part. For the purpose of analyzing the corrections to the polar geometry we shall take into account just the $\overline{B}_{iron}$ part.

3. Corrections to the pole tip geometry due to mechanical reasons

Some modifications to the pole tip geometry described above were necessary in order to fulfill mechanical design

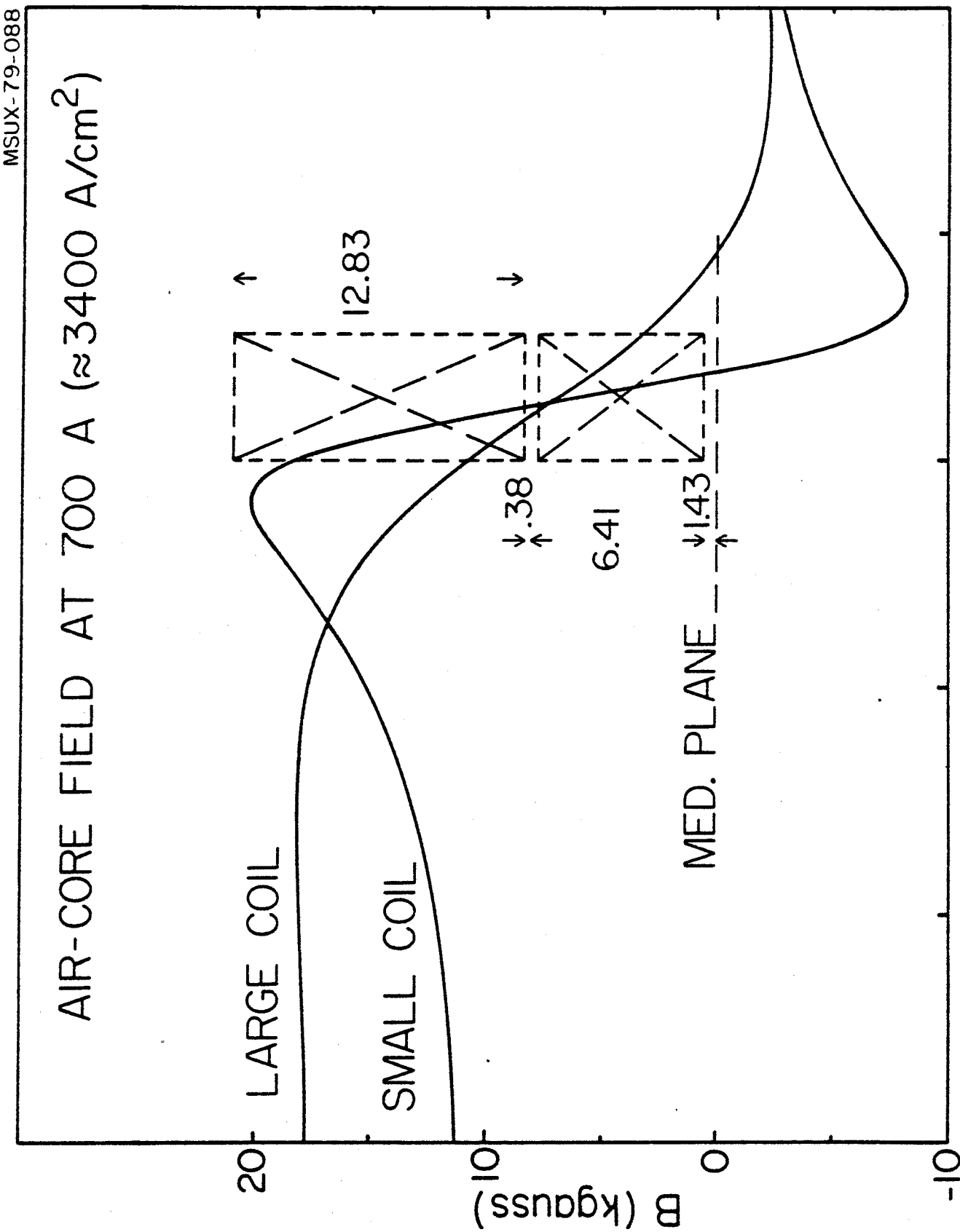

FIG. 3. Air core fields for the two main coil sections at 700 A. Coil dimensions in inches.

requirements not previously taken into account. There are three causes for this, as listed below:

- it was decided that the current leads of every trim coil, for every one of the three sectors, should be brought outside the cyclotron via axial holes tangent to the hills. Since there are 13 coils/sector, wrapped around the hills, this entices the drilling of 26 holes/sector, each one having a diameter of .75" as shown in Fig. 4. This solution is quite different from the one envisaged earlier, with the trim coils leads coming out along the dee stems holes in the valley, but it does simplify the mechanical problems. Its consequences on the field will be seen presently.
- the installation of the R.F. coupling and trimming capacitors, required the drilling of two holes/sector, of 3.5" diameter, centered at a radius of 23.75", i.e. near the outer pole radius, as shown in Fig. 4.
- an error in the axial clearance needed for the trim coils beneath the upper part of the hill allows to put an iron shim, of thickness .125", on top of the lower part of the hill, thus reducing by the same amount the gap between the two hill sections.

The consequences of these modifications were calculated by using the uniform saturation approximations, which has already proved successful in the plug design[2]. The results are shown in Fig. 5.

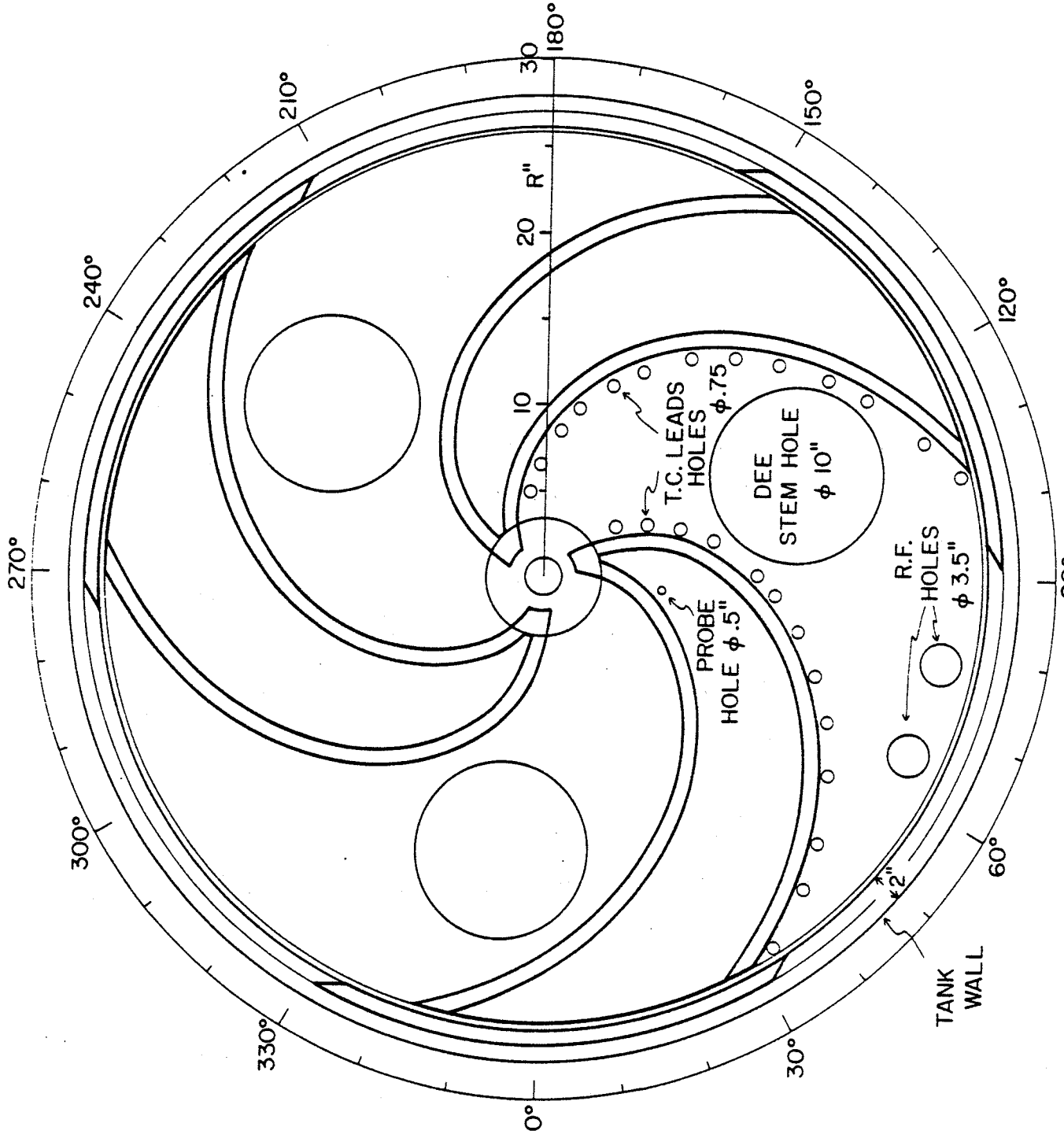

FIG. 4. Median plane view of the pole tip geometry.

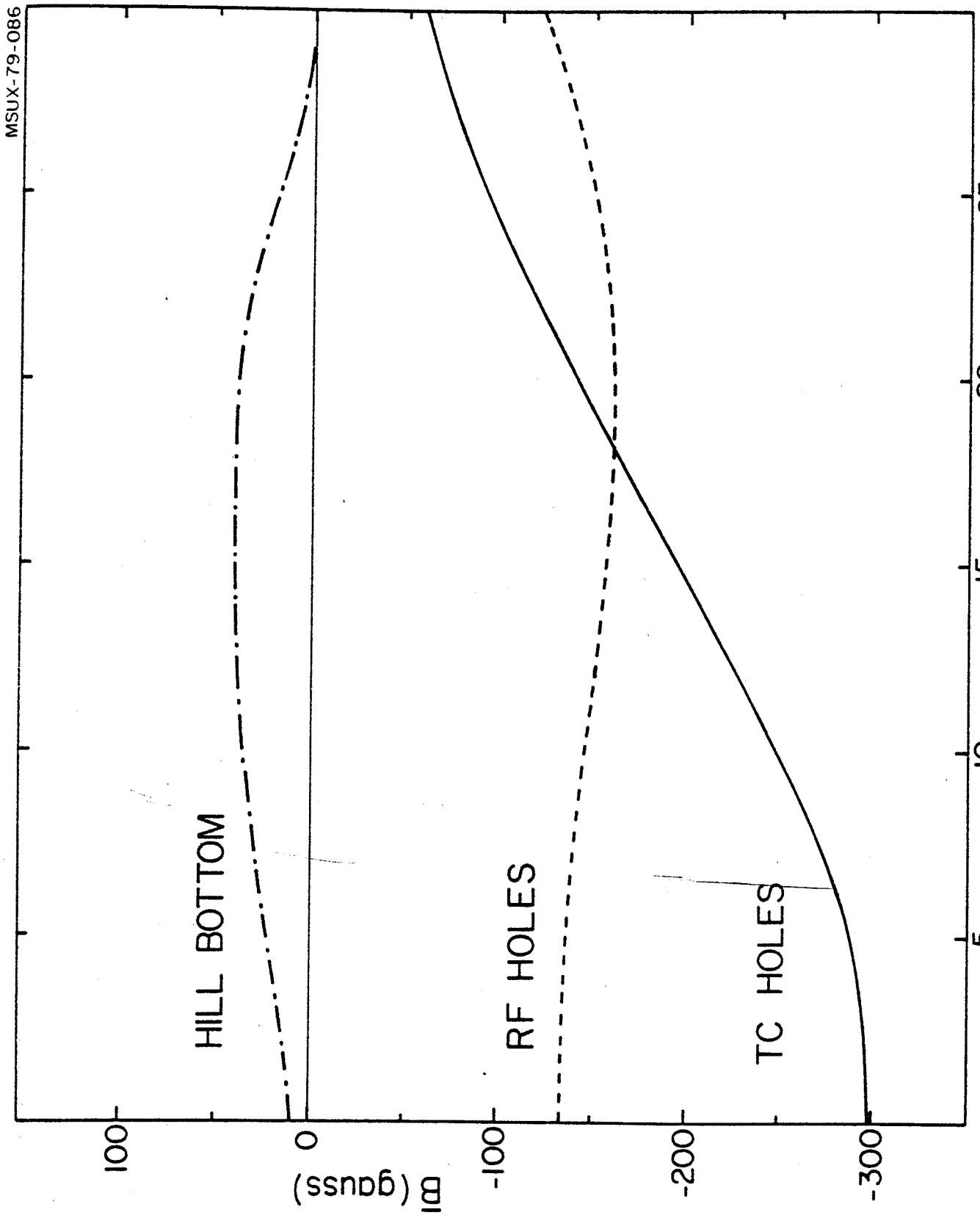

FIG. 5. Average field variations generated by the trim coils holes, R.F. holes and bottom hill shim. See text for details.

The average $\bar{B}_{iron}$ field, for the uncorrected geometry, measured at a coil excitation of I_α = 700 A and I_β = 198 A, is given by the solid line in Fig. 6. This excitation is close to the one needed for 80 MeV/n, Z/A = .5 particles, i.e. the most relativistic ones, which constitutes therefore a good test case for the actual machine performance. The dashed line in Fig. 6 shows instead the average field which may be expected as a result of the modifications described above.

Apart from the overall field decrease, there is a definite change in the average slope of the field itself, mostly due to the holes for the trim coils leads. We have checked in a number of cases that this change in slope would be sufficient to drive to very high levels the trim coils power needed for fitting the isochronous field. Furthermore, equilibrium orbit studies with the fitted field, and using the measured azimuthal field modulation showed that:

- the magnitude of the cone field at the center was slightly less than desirable, and a further increase in the cone field of about 100 gauss would be necessary.
- since the field modulation (see (2)) at the outer radii (22" to 26"), is less than the calculated one by $\sim$2%, the resulting flutter decrease makes the axial focusing in this region marginal for the most relativistic particles. In fact the loss in flutter could have prevented the cyclotron operation for 80 MeV/n, Z/A = .5 particles.

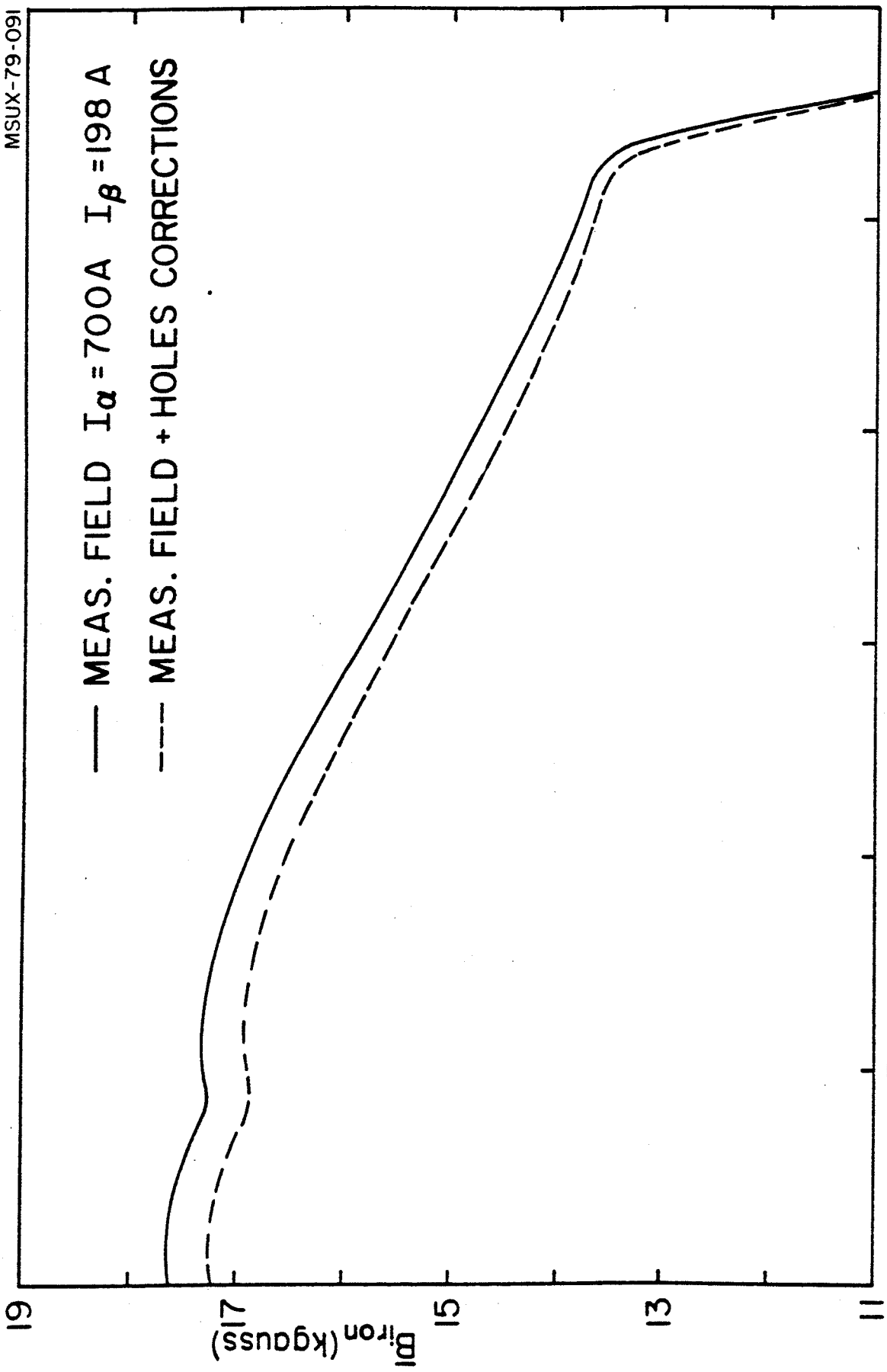

FIG. 6. Measured average iron field for the uncorrected pole tip geometry and expected field after drilling the holes. (See text for details.)

Consequently, both because of the construction reasons summarized earlier, and of the physical reasons just listed, it was decided that the pole tip geometry had to be corrected in several places.

4. Corrected pole tip geometry

All the evaluations of the corrections, being of quite local nature and generally close to the median plane, were made via the uniform saturation approximation.

The process of correcting a polar geometry, in view of achieving some predetermined field, is a painstaking trial and error procedure which has, in fact, no unique solution. Concerning this problem the advantage of a superconducting cyclotron with respect to a conventional one is the simplicity of the uniform saturation approximation and the reliability of the latter, at least for small corrections.

Our final results are shown in Fig. 7 both for the hill and valley profiles. We shall now review those corrections separately for the plug, the inner pole radii, and the outer radii. In what follows z indicates the distance of all surfaces from the median plane.

4.1 Plug

The desired increase in the field center bump was accomplished by decreasing the z of the cylindrical part by .15" between 1" and 1.5" radius, and by .37" from 1.5" to 2". Similarly in the hill part, z was lowered by .15" between 2" and 3"

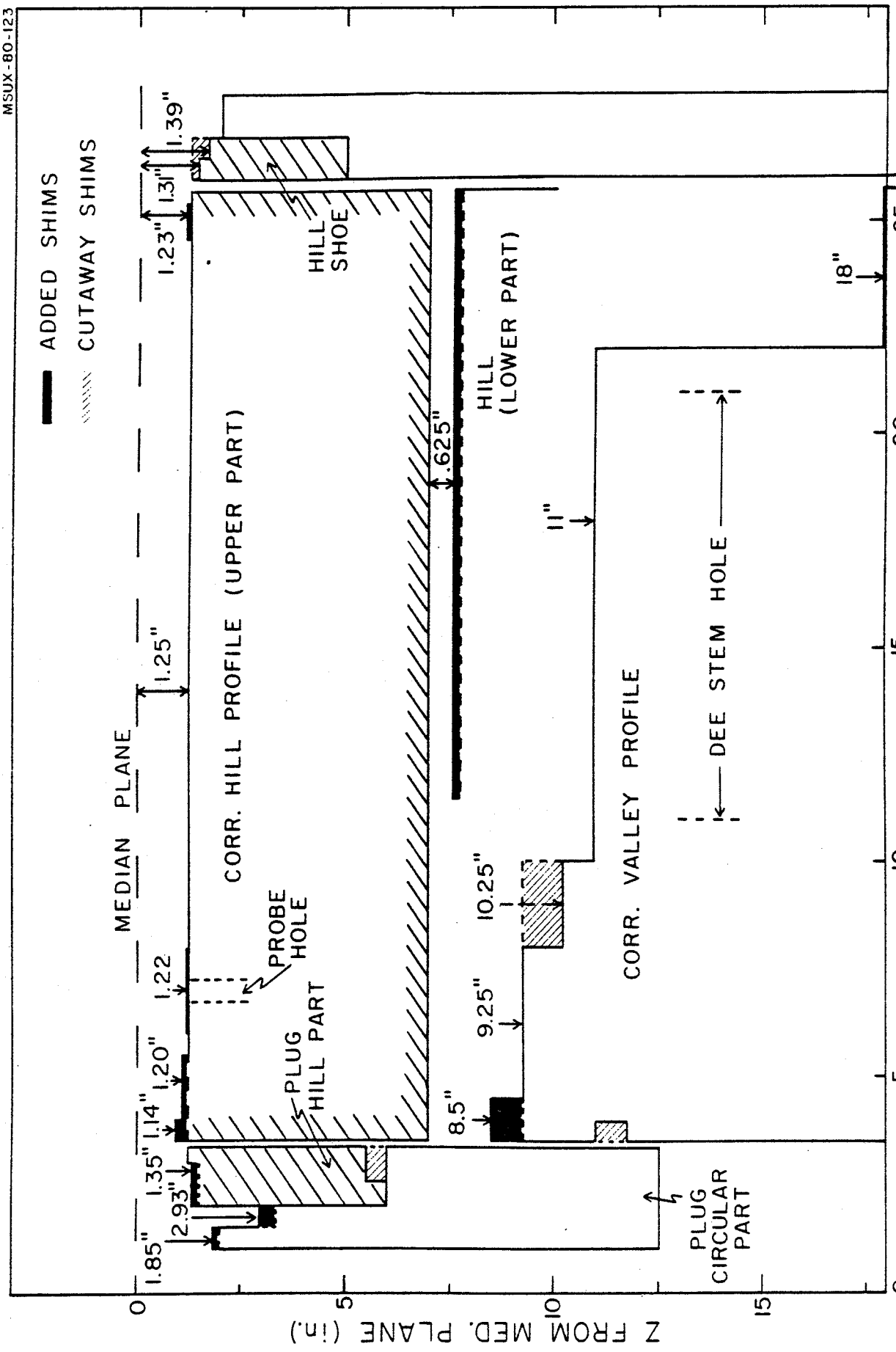

FIG. 7. Radial hill and valley profiles indicating all corrections (see text for details).

radius. In order to properly insert the plug two non magnetic rings are needed, one positioned at a z=6", and .5" thick between 2.54" and 3.32" in radius, which entails a slot on the hill part of the plug. The second, a centering ring, entails a circular slot in the pole structure, between 3.5" and 4", .75" thick and with z=11". In order to correct for these slots a shim has been added on the valley floor, from a radius of 3.5" to 4.5", where z changes therefore from 9.25" to 8.5". The total effect of these corrections is given by the solid line in Fig. 8, showing an average increase in field of about 200 gauss over the first 3" in radius.

4.2 Inner radii

In order to adjust the average field slope over the radial range of 5" to 15", the simplest solution was to cut off part of the valley shim, from 8" to 10" radius, for a thickness of 1". Given its distance from the median plane, z=9.25", its effect spreads over a very large radial range, as shown by the dot-dash line of Fig. 8. A shim on the hill was also needed around 4" in radius, where the undershot of the field produced by the plug corrections gives a field gradient which may jeopardize the axial focusing. This shim lays on top of the hill between 3.5" and 5" radius, and is therefore 33^{o} wide. Its thickness is 100 mils from 3.5" to 4", and 50 mils thereafter. Its effect on the field is shown by the dashed line of Fig. 8.

It was also decided that one hole/sector should be drilled through the hill, for inserting a phase defining slit. The

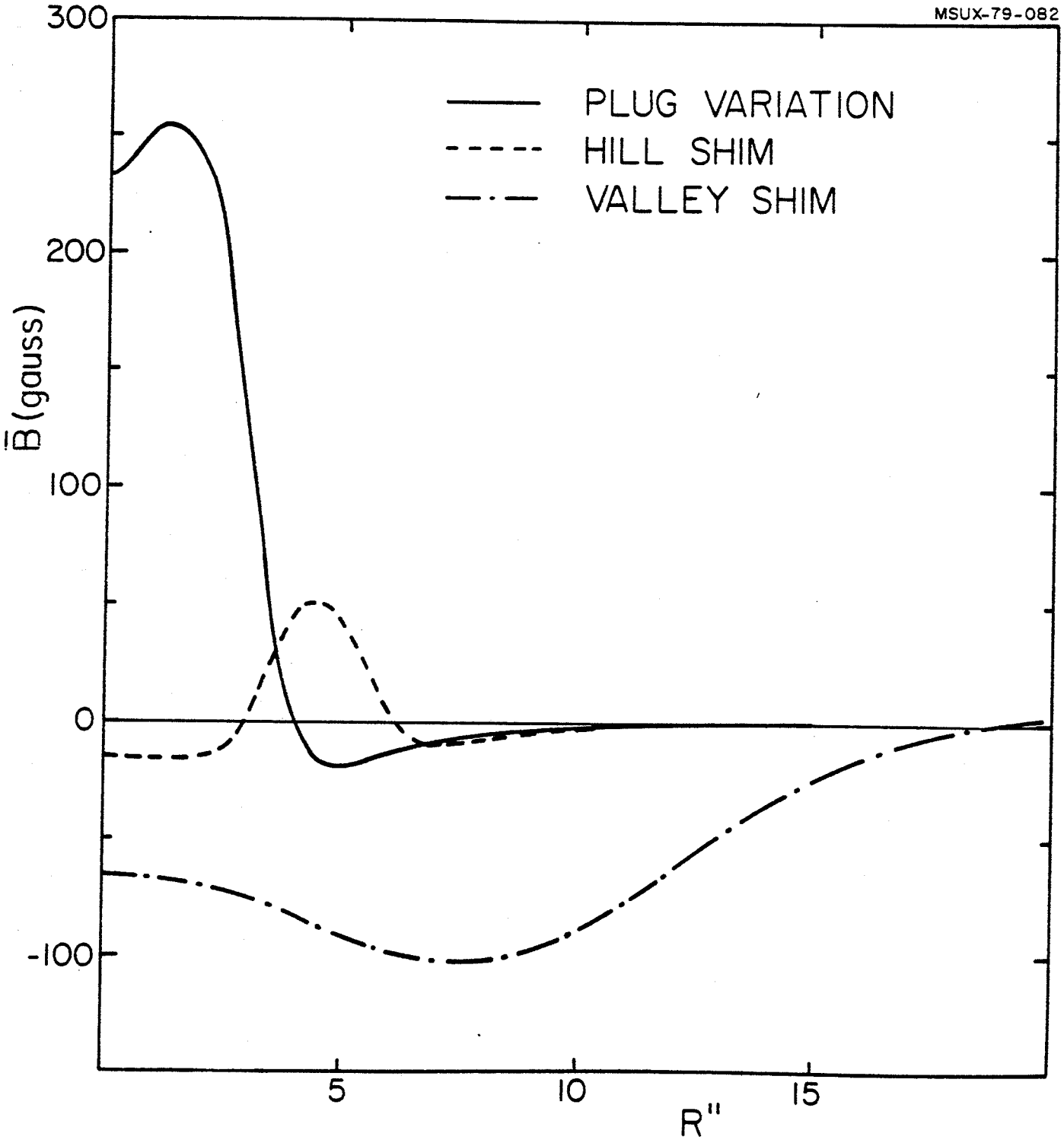

FIG. 8. Average field variations produced by the plug correction (solid line), the hill shim between 3.5" and 5" radius (dotted line) and the valley shim between 8" and 10" radius (dotted-dashed line).

hole, at a radius of 7" and .5" in diameter, has an effect on the average field as shown in Fig. 9. In order to compensate for it, the best shim we could design, taking into account the thickness limitation which comes from the axial dimensions of the trim coils, is a 30 mils thick slab lying on top of the hill and extending from a radius of 6" to 8". Its compensating effect is shown, with a reverse sign for the sake of comparison, by the dashed line of Fig. 9. The compensation is not perfect but leaves a rather smooth field which has no effect on the beam dynamics.

4.3 Outer radii

The need for assuring adequate axial focusing at radii around 25" proved to be the most lengthy task. Axial clearance problems for the trim coils make it impractical to restore the focusing by shimming the hill locally, so as to increase the flutter.

We therefore chose to alter locally the average field gradient. Since the trim coils are not properly positioned to produce the required field variation, shims had to be devised.

A number of solutions were tried, and the one chosen consists of:

- a 20 mils thick shim from 24.6" to 25.5", located on top of the hill and about 40° wide. Its effect on the field is shown by the dashed curve of Fig. 10.
- a step-like reduction of the hill shoe height, located between 26" and 27" in radius. Its height has been reduced

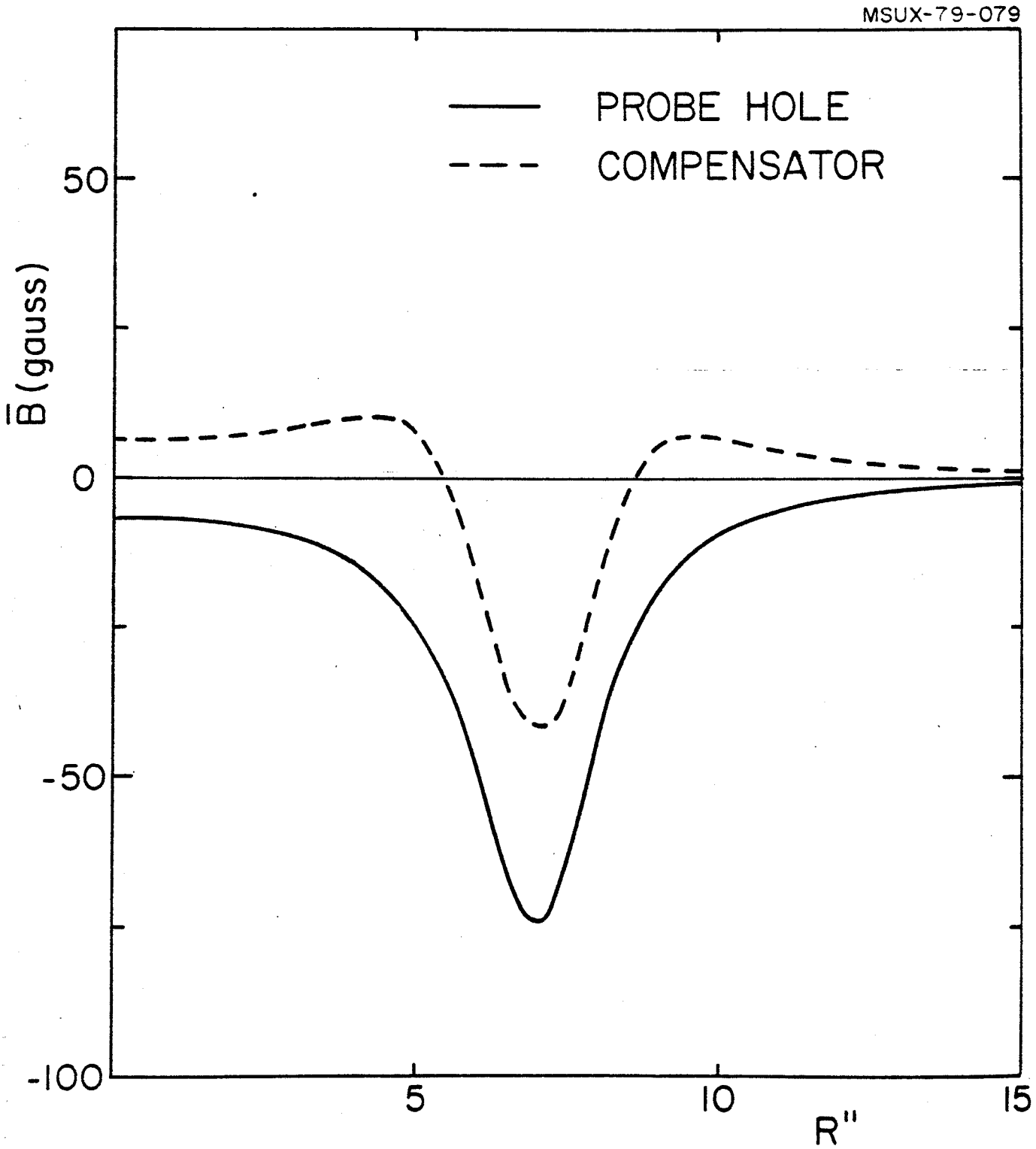

FIG. 9. Average field variation produced by the probe hole and its compensating shim. The latter is shown with reverse sign.

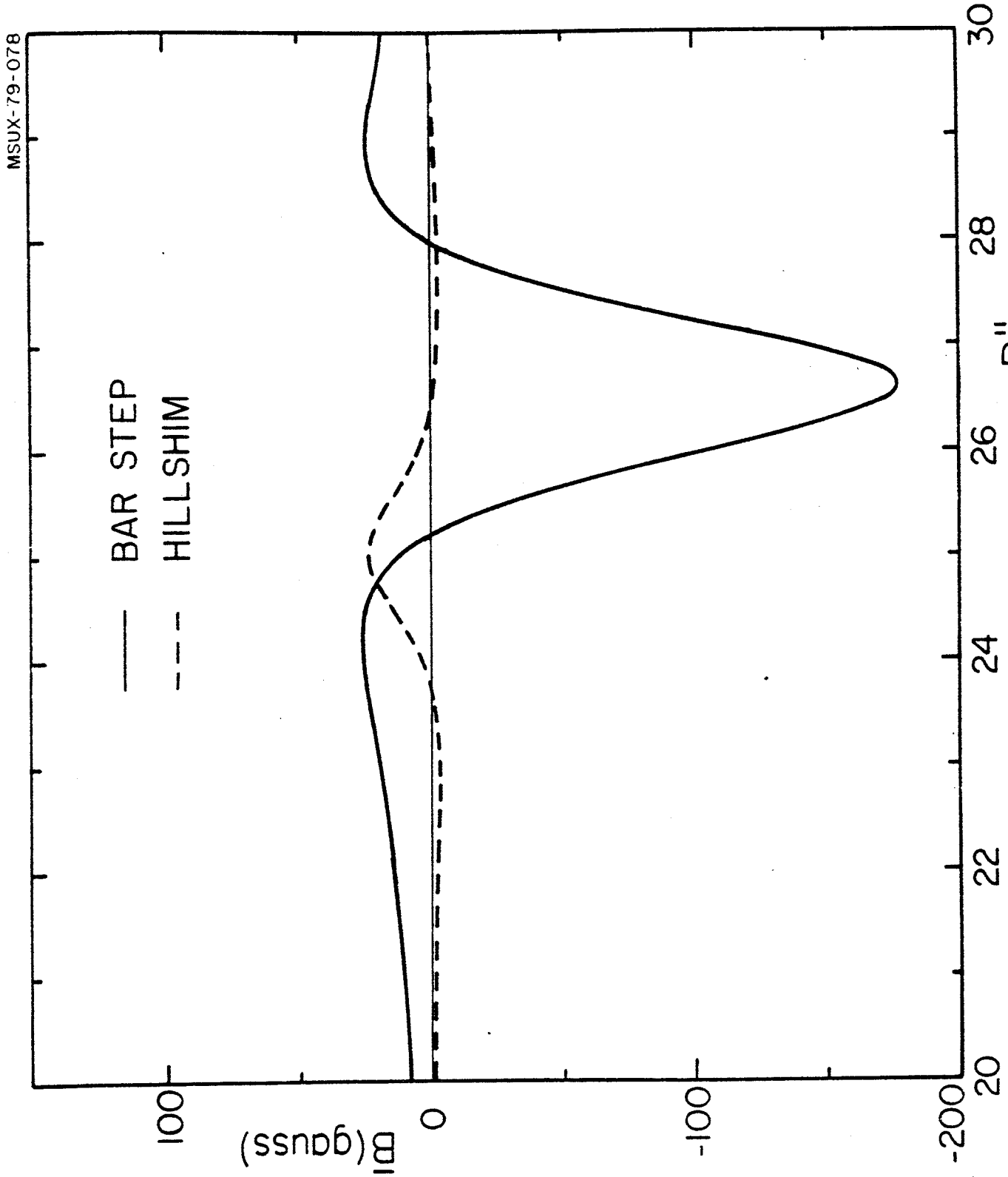

FIG. 10. Average field variation produced by the hill shim and the hill shoe corrections. See text for details.

by 60 mils between 26" and 26.5", and by 140 mils between 26.5" and 27". The resulting field correction is shown by the solid curve of Fig. 10.

When all these corrections are summed up, one obtains a field which is shown by the solid line of Fig. 11. A comparison can be made against the dashed curve, which represents the measured field at I_α = 700A, I_β = 198 A, plus the contributions of trim coils holes, R.F. holes etc., as previously shown in Fig. 6. One can quickly note the enhancement produced by the plug, the average slope variation introduced by the valley cut and the drastic change in the field fall-off near the pole radius.

These corrections obviously affect also the field modulation. The computed effect has been added to the measured modulation and inserted in the fully self-consistent calculations which are discussed in the following.

5. Main aspects of the cyclotron performance

5.1 Computing methods

The present calculations involve a two step process:

- generation of a magnetic field map, for the ion to be studied.
- analysis of the equilibrium orbit properties via a normal E.O. code.

It is worthwhile to briefly review the procedures used in the first step, because they implied the writing of a pre-

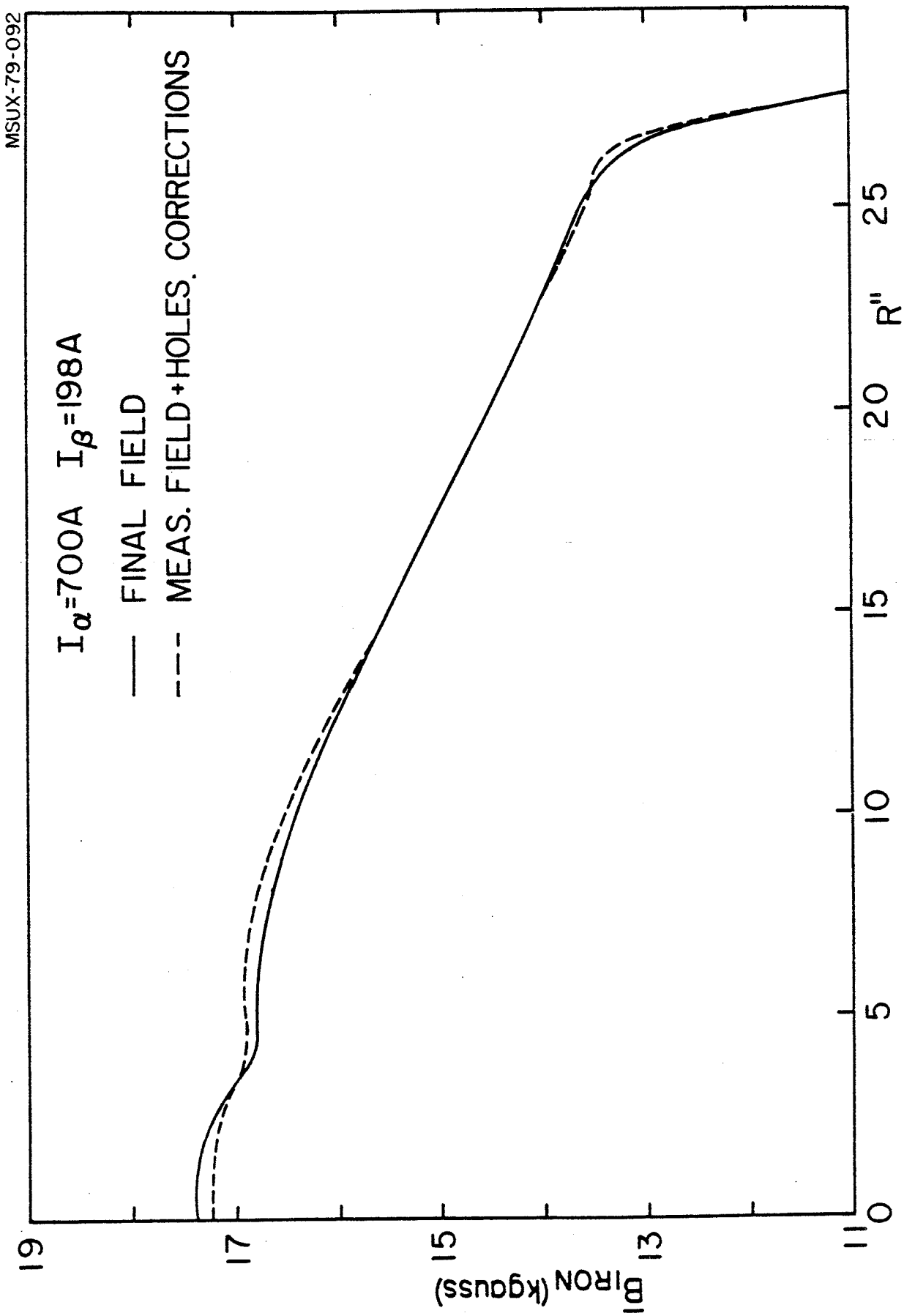

FIG. 11. Expected final average field at I_α=700 A, I_β = 198 A (solid line). The effect of the shims can be seen by comparison with the dashed line. See text for details.

viously unavailable code. These notations will be used throughout: Z/A, charge to mass ratio of the ion studied; Bo, nominal center field value of the map for which the isochronous field is calculated; T/A, ion energy in MeV/nucleon.

A typical magnetic field map for the K-500 cyclotron has a radial grid mesh of 0.5", from r=0" to r=40", at azimuthal steps of 1^{o} over a 120^{o} sector. Such a map is obtained by superposing the average field to every point of a modulation map (either calculated or measured), i.e. a map where the average field is zero at all radii. The modulation map is kept constant during the computation, since the introduction of the experimental variations of the modulation with the magnet excitation[2] would be too cumbersome for the present purposes, and they are rather small anyway.

The average field at any radius is generated by fitting either the isochronous field, for a given Z/A and Bo values, or any externally supplied field. The fitting is done via a standard least squares procedure.

The elements which enter in the fitting procedure are:

- $B_{is}(r,Bo,Z/A)$ i.e. the isochronous field, or any externally supplied field. In the case of the isochronous field the latter is computed by the code using the relevant harmonics of the modulation map up to order 15th and an iterative procedure. We have checked the accuracy of the procedure against E.O. data and found it better than $\pm\ 3.10^{-5}$.

- the main coil air-core fields shown in Fig. 3.
- the air-core trim coil fields, some of which are shown in Fig. 12 for a current of 300 A. The 13 trim coils are made by two layers of 5 turns each of .25" square hollow copper conductor, and are approximatley equally spaced from 3.5" to 25" radius.
- the measured $\bar{B}_{iron}(r)$ at 23 different values of (I_α, I_β)[1] to everyone of which the calculated correction discussed above were added.

Even though the fitting is via a standard least square procedure, since the $\bar{B}_{iron}(r)$ is a function of (I_α, I_β), an iterative procedure had to be followed. An initial fitting is done by using the $\bar{B}_{iron}(r)$ at a guessed value of (I_α, I_β). Afterwards, the $\bar{B}_{iron}(r)$ is recalculated using the I_α, I_β given by the fit, and the procedure repeated until the difference between the two successive I_α, I_β, values is typically less 0.1 A (0.01% - 0.02%). The iteration is converging very rapidly never requiring more than 4-5 iterations whatever the initial guess of (I_α, I_β). The calculation of the $\bar{B}_{iron}(r)$ at any point of the (I_α, I_β) grid is done by least squares fitting of a 3rd order polynomial in (I_α, I_β) over the 16 known points closest to the desired point. Its accuracy, as checked with actual measurements, is better than 0.01%. The fit can be done either with all trim coil currents free, or setting limits on their individual values, or on the max. trim coil power.

The ultimate result of the fit to the isochronous field are the values of I_α, I_β, the corresponding $\bar{B}_{iron}(r)$ and the

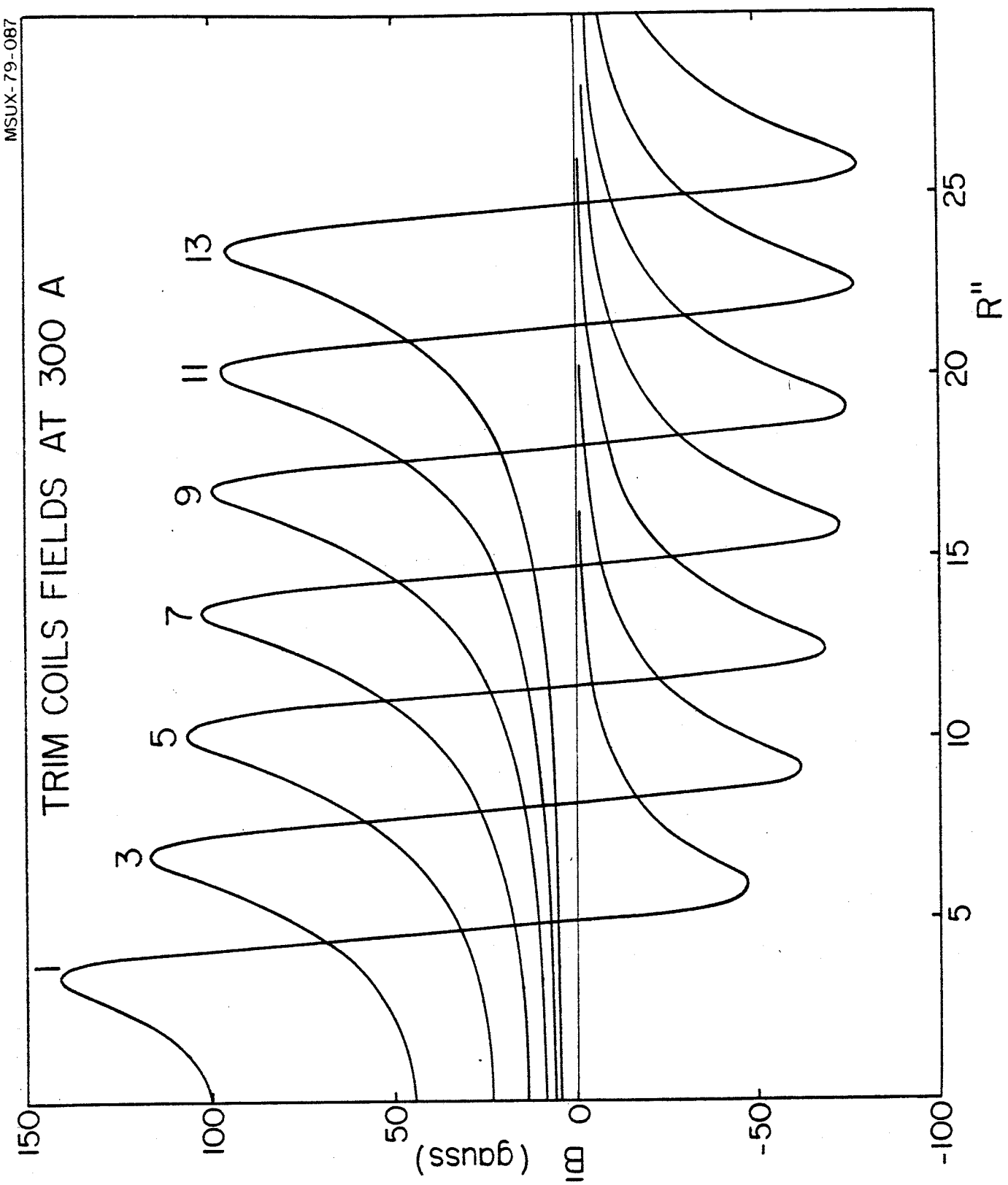

FIG. 12. Air core average field at 300 A for the indicated trim coils.

trim coil currents. A total average field as a function of the radius can thus be calculated and added point by point to the modulation map.

All the calculations presented here use the measured modulation map at I_α = 700 A and I_β = 298 A, to which the one produced by the corrections discussed above have been added. These I_α, I_β values were chosen because of their proximity to the focusing limit, wehre flutter deficiencies are more critical.

In summary the resulting picture of the K-500 field is very much self consistent and accurate.

5.2 Cyclotron operating range and fitting results

The overall operating range of the machine in the (B_o, Z/A) plane is shown in Fig. 13. The range if limited by the 50 kgauss field at extraction (bending limit, K=500), by the focusing limit K_{FOC}=160 ($T/A = K_{FOC}\ Z/A$), the Z/A = .5 line and the low field limit B_o = 30 kgauss. The latter derives from the existence of the $\nu_R + 2\nu_z$=3 resonance which, at low fields, prevents the beam from reaching the extraction radius without large axial blow-ups. This aspect for the K-500 cyclotron is described in more detail in (3). As for the two Z/A > .5 particles, i.e. $^3He^{++}$ and protons, it appears that the machine would probably work only marginally because of the low field required.' We have therefore chosen not to consider them.

On the same (Bo, Z/A) plane one can draw the lines corresponding to constant values of I_α and I_β, as obtained by

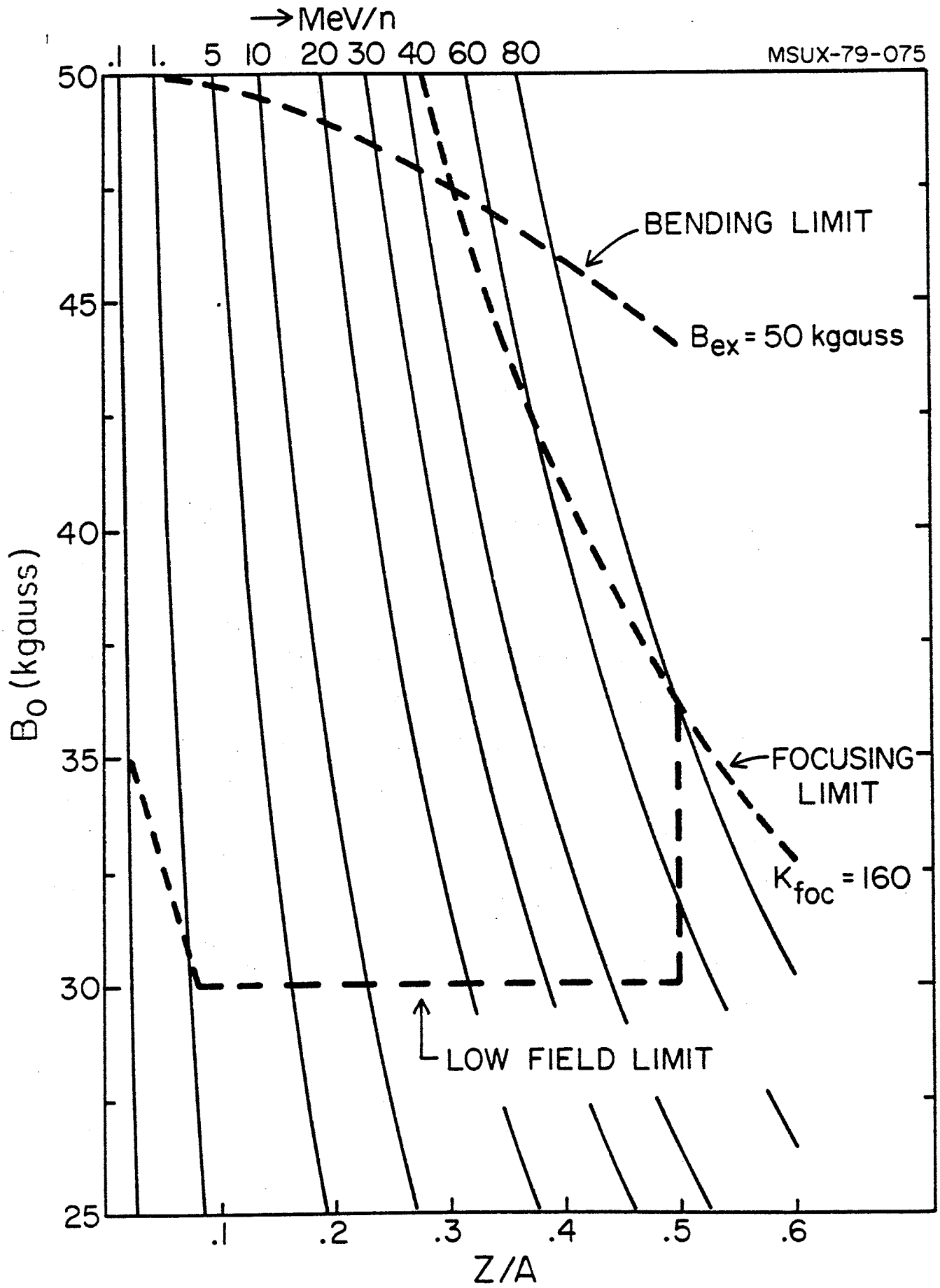

FIG. 13. Operating diagram of the K-500 cyclotron in the (Bo, Z/A) plane. Also indicated are the lines of constant energy.

actual fitting of the isochronous field in a number of cases. This is shown in Fig. 14. The K-500 cyclotron needs therefore a current I_α in the small coil ranging between 450 A and 800 A, while I_β is between 150 A and 750 A. These higher than the design values (I_{design}= 700 A) have been run in actual measurements,[2] and no problems encountered.

The consequent operating diagram of the cyclotron in the (I_α, I_β) plane is shown in Fig. 15. The boundaries corresponding to the bending limit, K=500, the focusing limit (K_{FOC}= 160) and the minimum Z/A and B_o values are well defined. Lines with constant B_o and Z/A are also shown.

The same fitting calculations which provide this picture of the (I_α, I_β) operating range also yield a detailed picture of the trim coil requirements. This is shown in Fig. 16 where the lines corresponding to a constant total trim coil power are drawn. The calculated power does not include leads resistance, power supply losses etc. In the upper left corner of the operating range, i.e. high fields and very small Z/A, the currents of some trim coils have been limited to 400 A, with no prejudice however, as will be seen later, for beam dynamics properties. This stems from the fact, as a glance to Fig. 13 confirms, that this region ocrresponds to very low energies, i.e. small turn number, and will in fact be used only when the K-500 cyclotron operates as injector for the K-800 cyclotron.[4]

The pattern of the trim coil currents varies considerably over the operating range even though the total power may be the same. This is of course expected, since the requirements

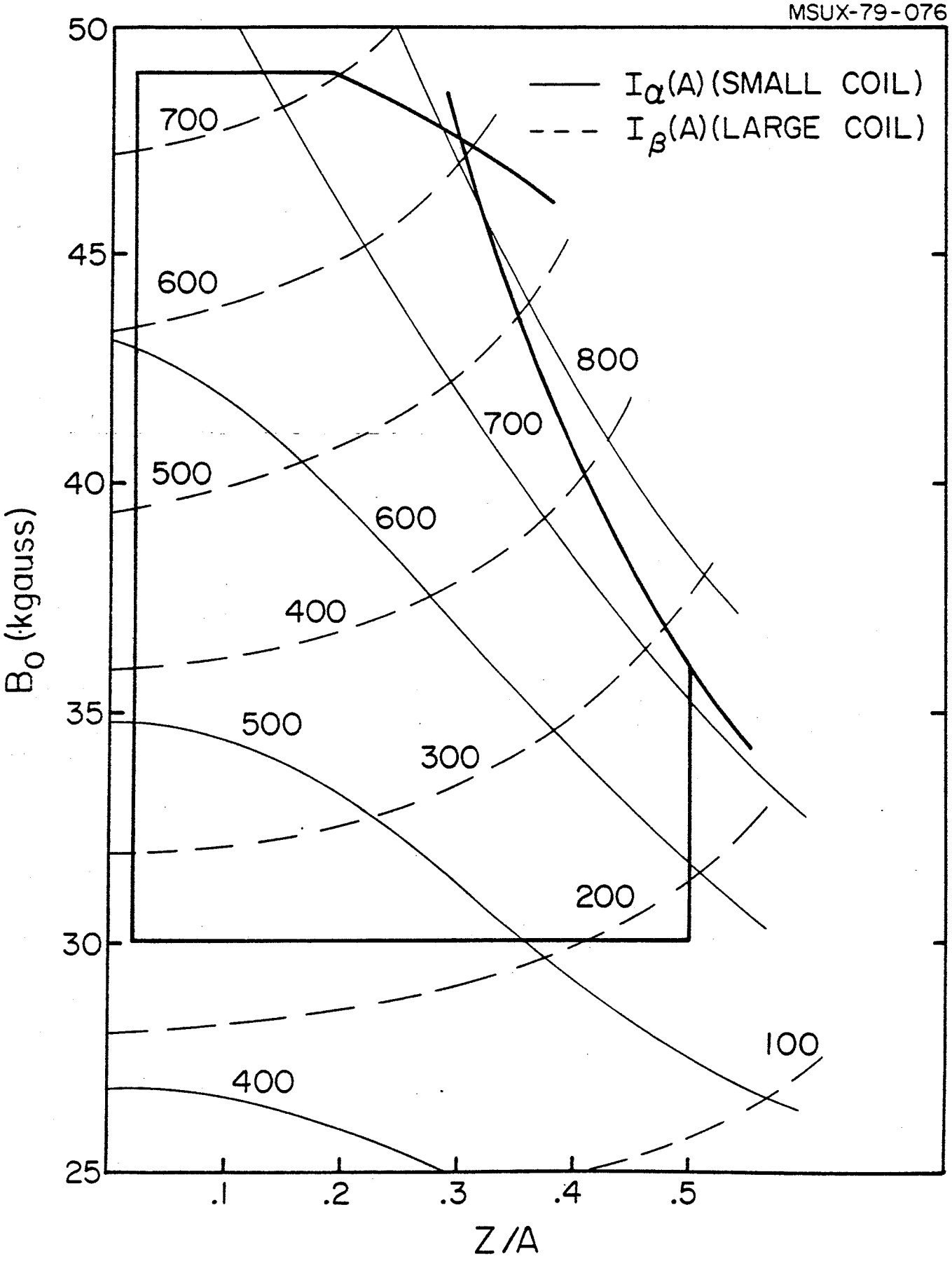

FIG. 14. Constant I_α and I_β current contours for the K-500 operating range in the (Bo,Z/A) plane.

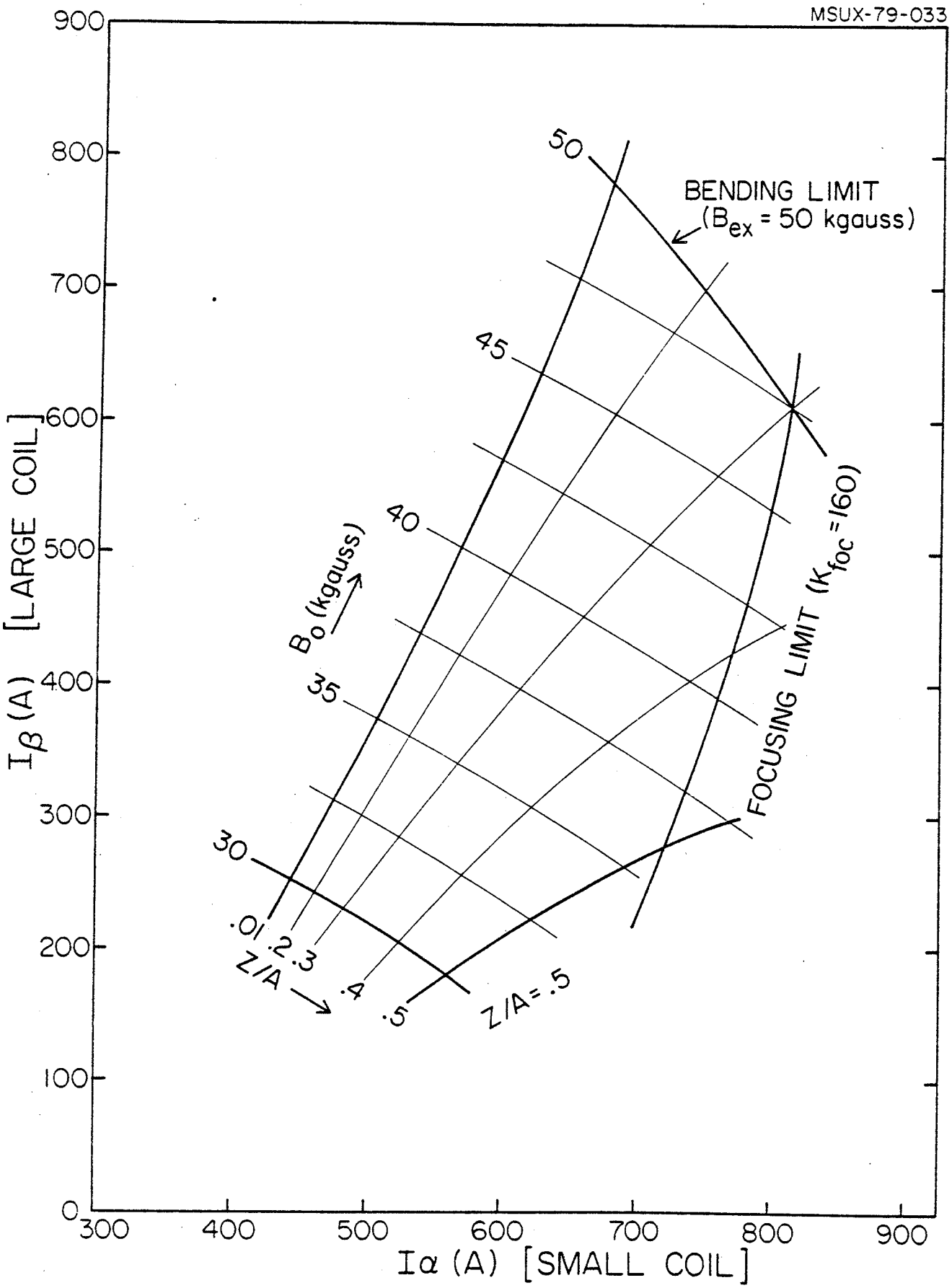

FIG. 15. Operating diagram of the K-500 cyclotron in the (I_α, I_β) plane.

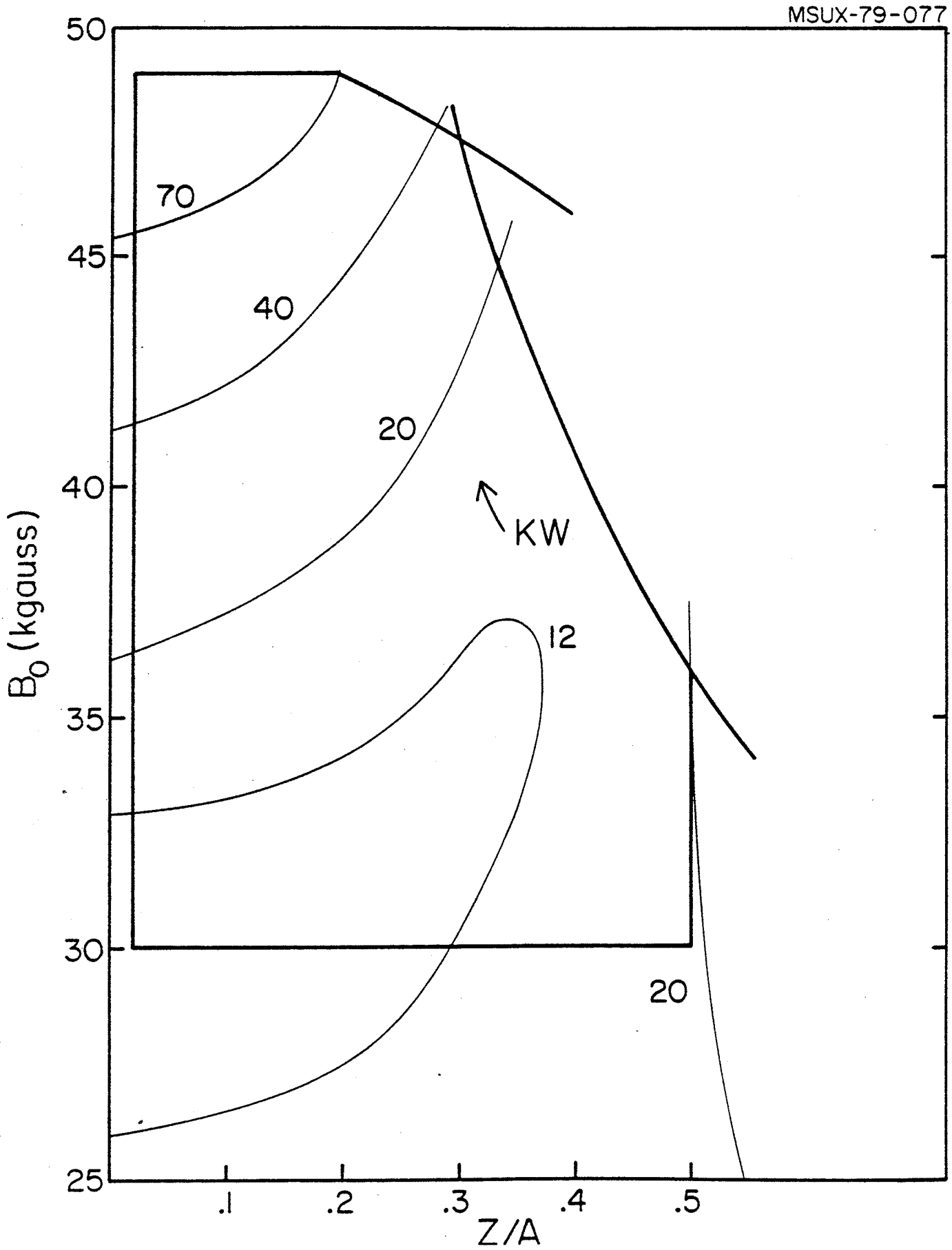

FIG. 16. Constant trim coils power contours for the operating diagram of the K-500 cyclotron in the (Bo, Z/A) plane.

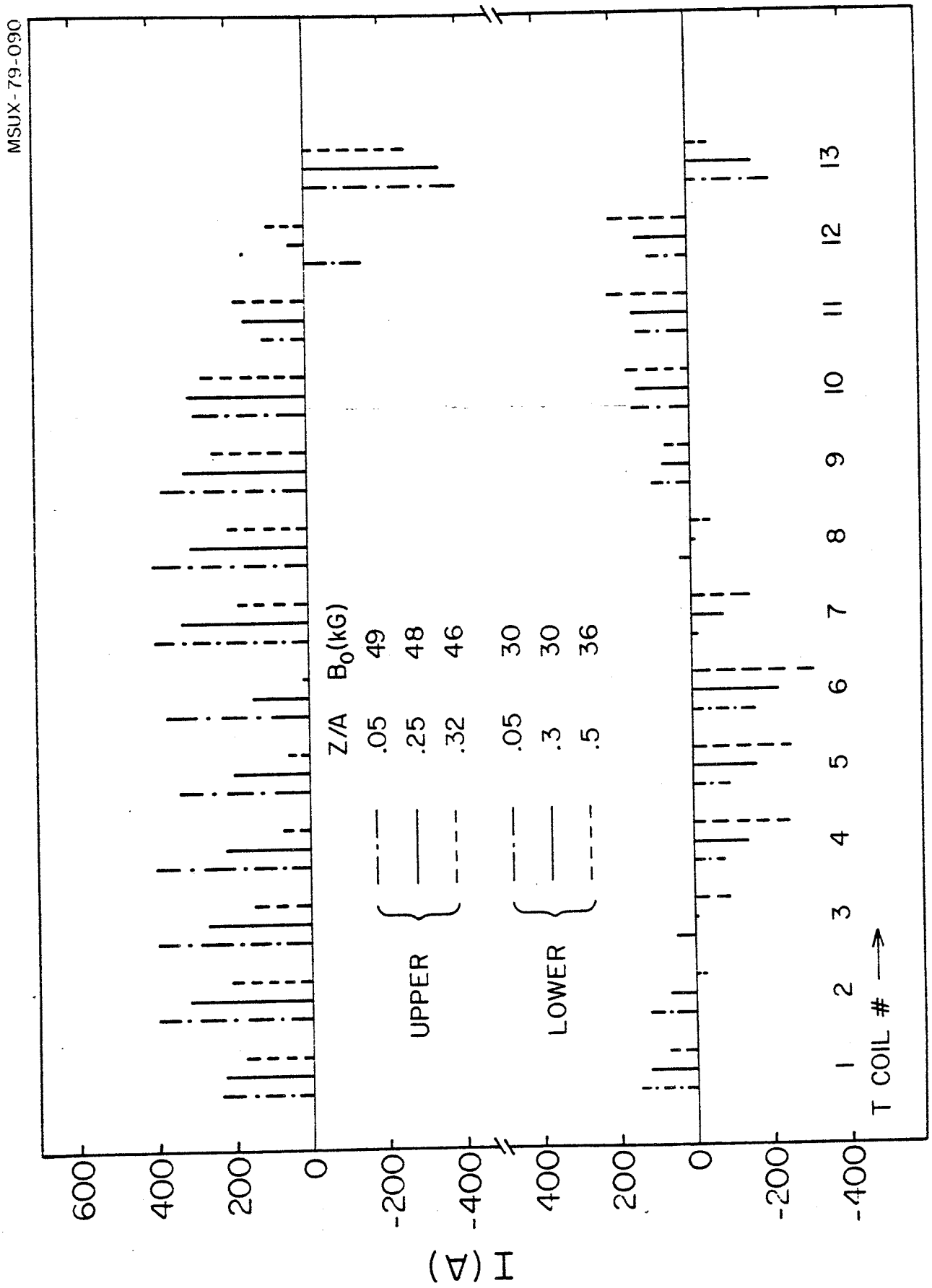

FIG. 17. Trim coil currents for six representative ions.

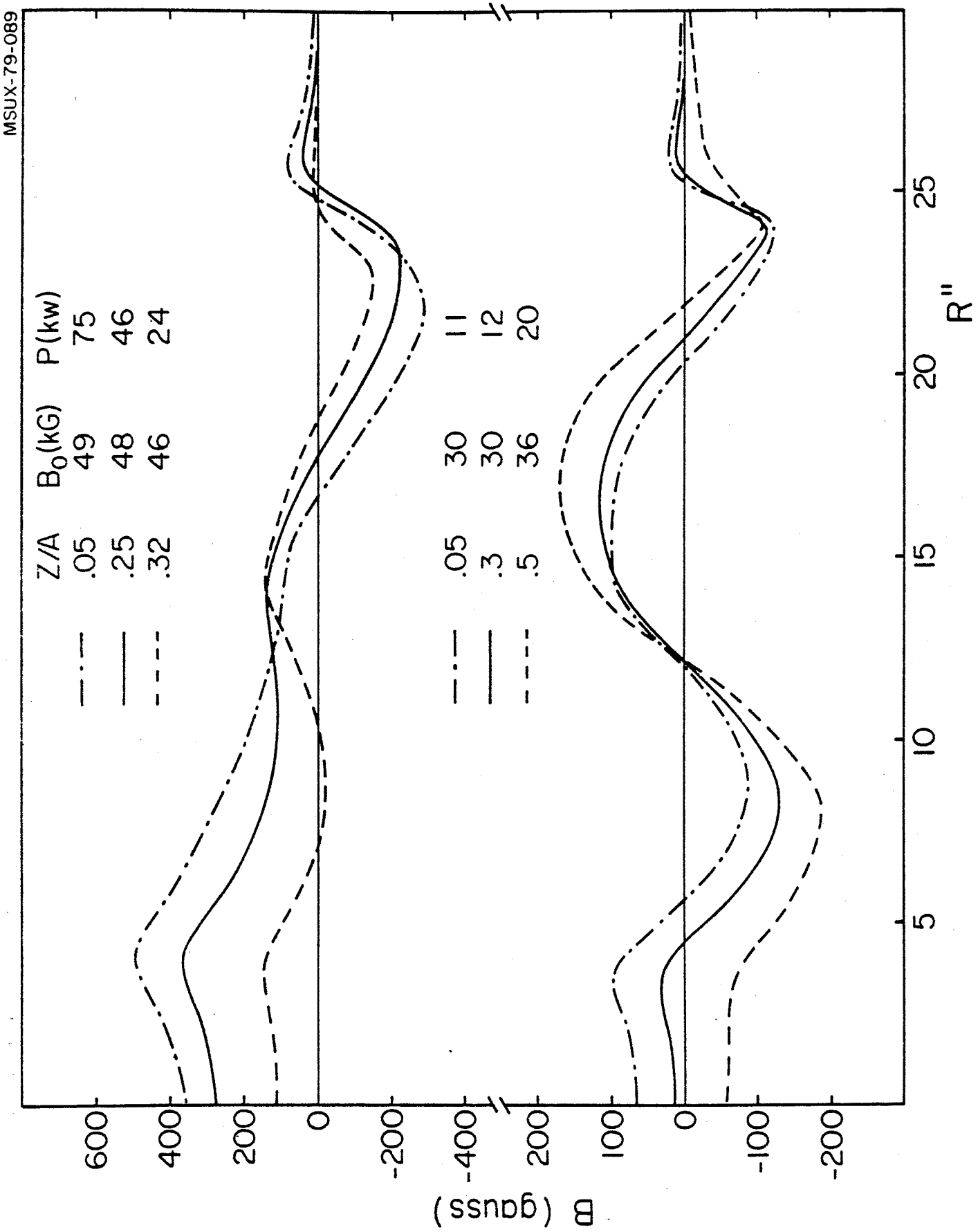

FIG. 18. Trim coil field contributions for six representative ions.

for the isochronous field vary considerably, i.e. from a very flat field at low energies to strongly radially increasing fields at high energies. An example of the current patterns for all 13 trim coils is presented in Fig. 17 for 6 representative ions, which can be identified along the contours of the operating diagram of Fig. 13. The total trim coil contributions to the fields are shown, for the same six ions, in Fig. 18.

These results confirm that a maximum current of 400 A in each trim coil is sufficient to achieve isochronism over the entire operating range of the K-500 cyclotron.

5.3 Equilibrium orbit properties

As an example of the overall performances to be expected from the cyclotron we will discuss the equilibrium orbit properties for eight ions chosen along the contour of the operating diagram of Fig. 13.

The total average field, ν_z and phase for Z/A = .5 ions are shown in Fig. 19 for the two cases B_o = 36 kgauss and B_o = 30 kgauss. They correspond to deuterons, alphas or any other fully stripped light ion with extraction energies of 80 MeV/n and 53 MeV/n respectively. Note that the first case is on the focusing limit line, K_{FOC}= 160. For both ions the chosen starting phase is around $+25^o$, as indicated by center region studies,[5] and drops to 0^o at 4", because of the presence of the magnetic cone. The phase then hovers around 0^o for most of the accelerating cycle, confirming the very

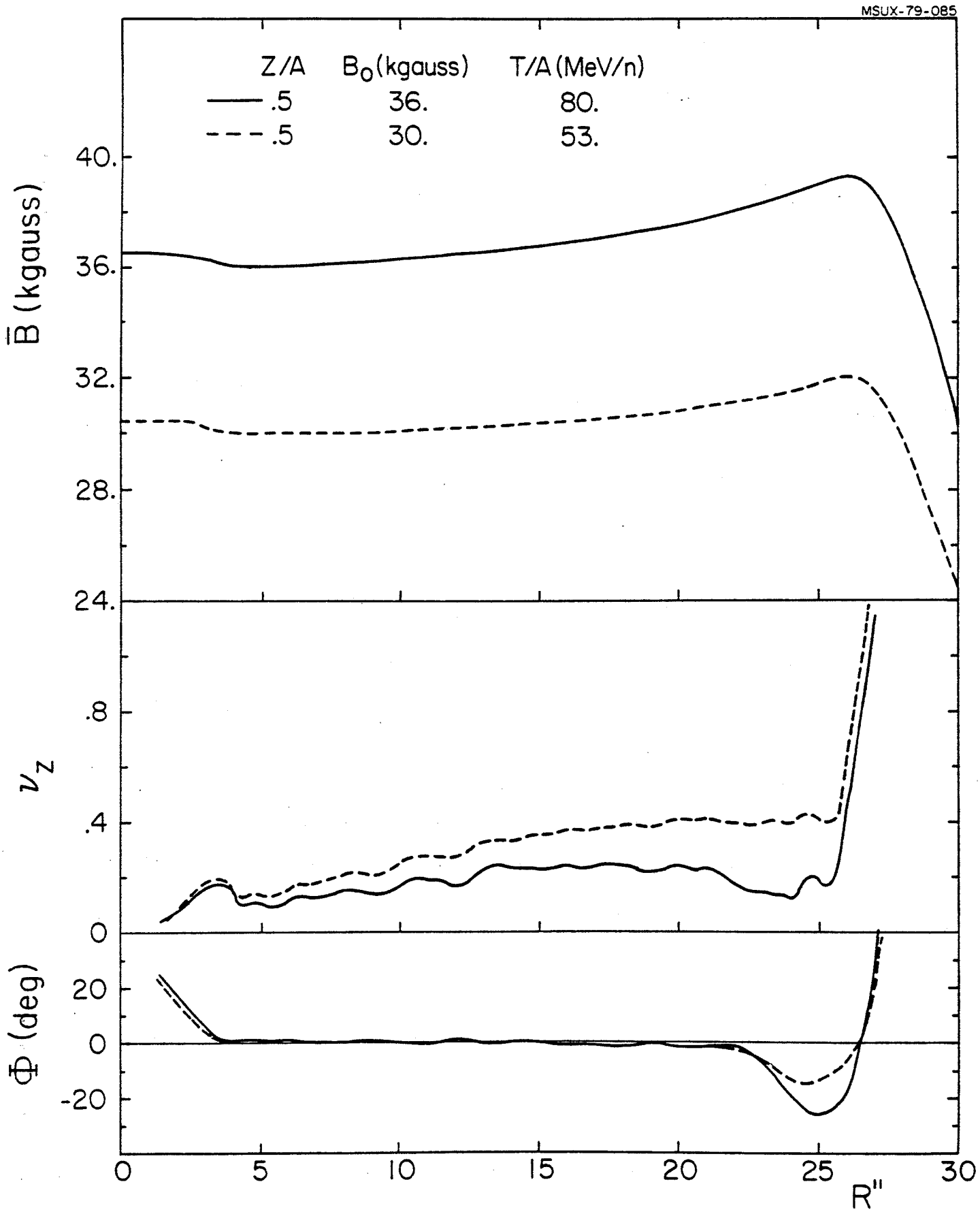

FIG. 19. Average field, ν_z and phase, as a function of the radius, for an ion with Z/A=.5 and center field level of 30 and 36 kgauss.

high degree of isochronism of the field. Note however the presence of oscillations in the ν_z curve, more pronounced in the high field case than in the low one. They are generated by the trim coils and correspond to local field gradients above or below isochronism. Although much less apparent they exist in the phase as well. The physical reason of these field oscillations is the shape of the trim coils form factors (see Fig. 12), and they are the more pronounced the higher the trim coil current. Their total number is equal to the number of trim coils.

For the same ion the field level decrease from 36 to 30 kgauss generates a considerable increase of the flutter and therefore of ν_z as shown by figure 19. Prior to the extraction radius, the fitted field is actually above isochronism, as can be readily seen from the phase curve which shifts towards negative values. This provides a phase closer to 0^o at extraction and keeps the minimum ν_z value at around 0.1 for the 80 MeV/n beam.

The analogous data for an ion with Z/A = .322, in the high and low field limits of 45.5 and 31 kgauss, are plotted in Fig. 20. The energies are 50 and 22.2 MeV/n respectively. This ion is fairly representative of a number of possible light ions beams, like $^{12}C^{4+}$ (Z/A=.333), $^{16}O^{5+}$ (Z/A=.312), etc. and is rather interesting from the machine point of view because in the high field case is very close to the rigidity limit (K=500) and focusing limit (K_{FOC}=160). The curves of Fig. 20 show that again the minimum ν_z is around 0.1, with acceleration above isochronism prior to extraction.

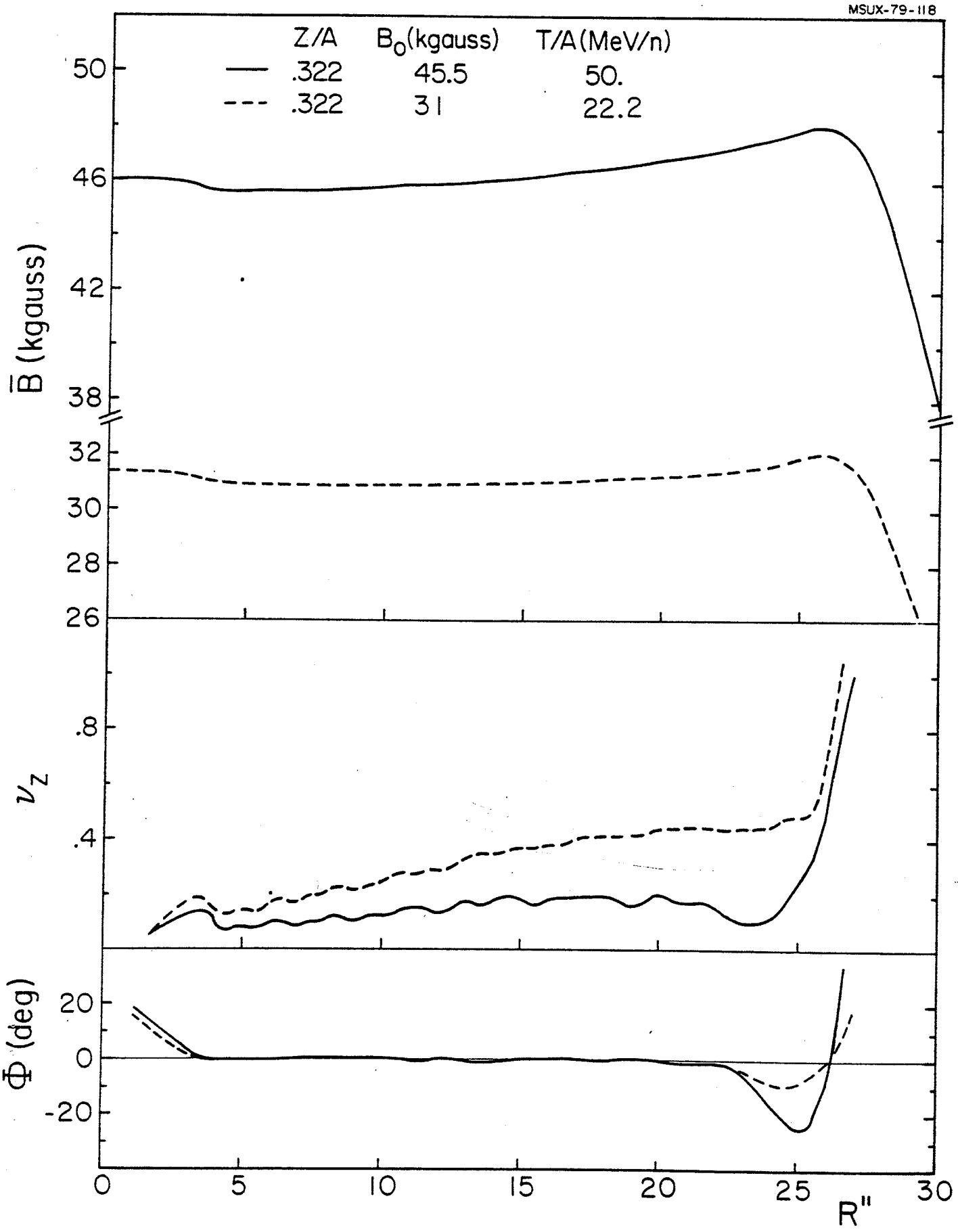

FIG. 20. Average field, ν_z and phase, as a function of the radius, for an ion with Z/A=.322 and center field level of 31 and 45.5 kgauss.

At the low Z/A end of the operating range, the data for a Z/A=.05 ion in the two cases of Bo=49 kgauss and 30 kgauss are presented in Fig. 21. The energies of these beams are 1.3 and .5 MeV/n respectively and correspond therefore to heavy ions beams in the injector mode, e.g. $^{238}U^{12+}$ (Z/A=.050), $^{208}Pb^{10+}$(Z/A=.048), etc. The average field is practically flat and the ν_z values are quite high, generally well above 0.2. It will be noted, however, that the oscillations in ν_z persist, and are quite evident in the high field case. This is due to the fact that even though the demands on focusing are reduced (henceforth the large average ν_z), this is a high trim coil power case and therefore a high current one as Figs. 17 and 18 confirm. The trim coils induced gradients are therefore large.

We also present in Fig. 22 two intermediate cases, one on the K=500 boundary, Z/A=.2 Bo=49 kgauss, and the other on the K_{FOC}=160 line, Z/A=.4 Bo=41 kgauss. The energy of the first is 21.2 MeV/n and it may correspond to a number of moderately stripped ions, e.g. $^{40}Ca^{8+}$, $^{20}Ne^{4+}$, etc. The second is a highly stripped light ion with energy of 64.5 MeV/n. The comparison between two beams of different Z/A shows an important aspect which is more apparent here than previously, namely the radial shift of the average field peak. As seen from the plots in Fig. 22, the peak shifts more inwards the least relativistic the particle. This is caused by the very different I_α, I_β settings needed for the two ions (as apparent from Fig. 15). It has the consequence that the outer

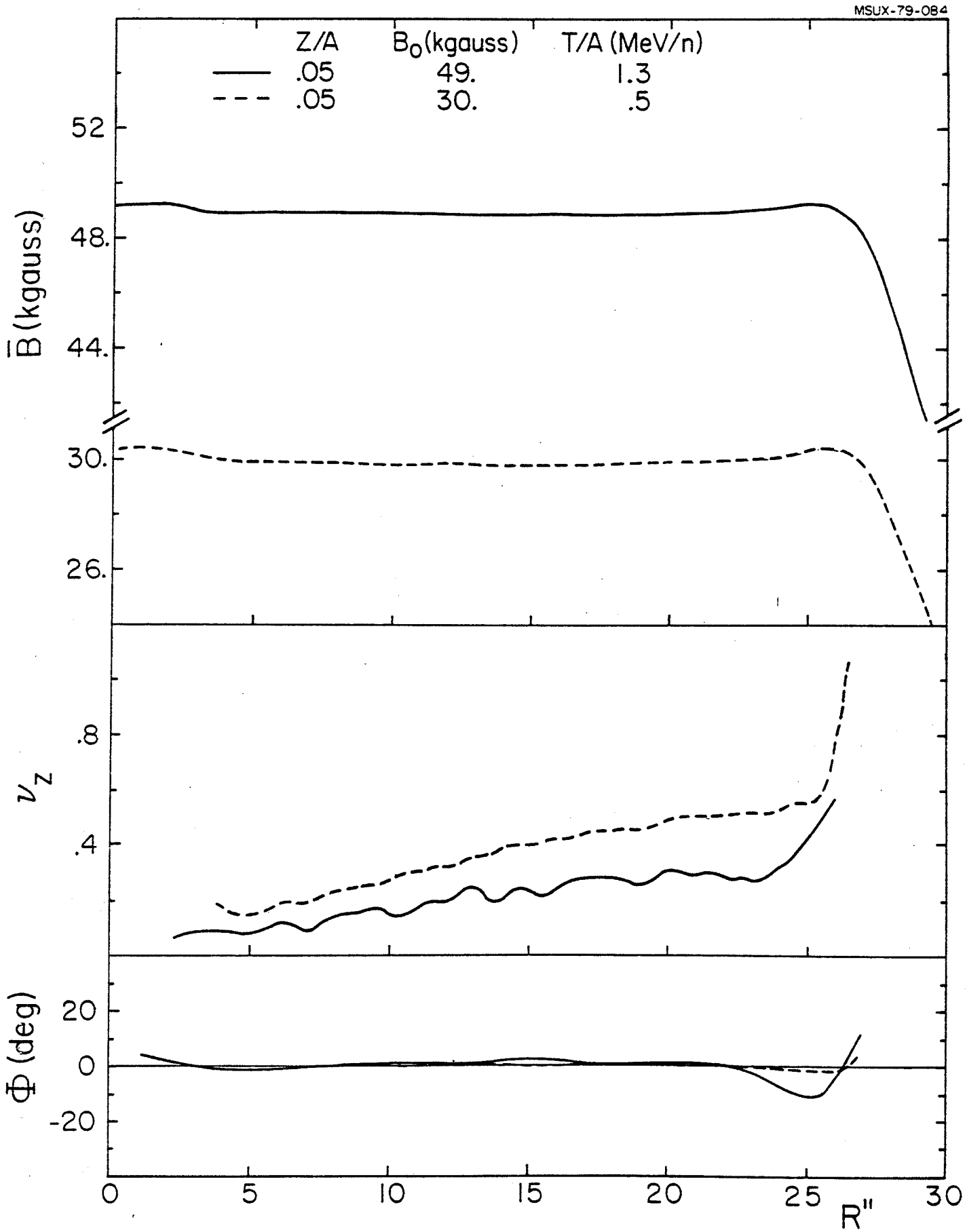

FIG. 21. Average field, ν_z and phase, as a function of the radius, for an ion with Z/A=.05 and center field level of 30 and 49 kgauss.

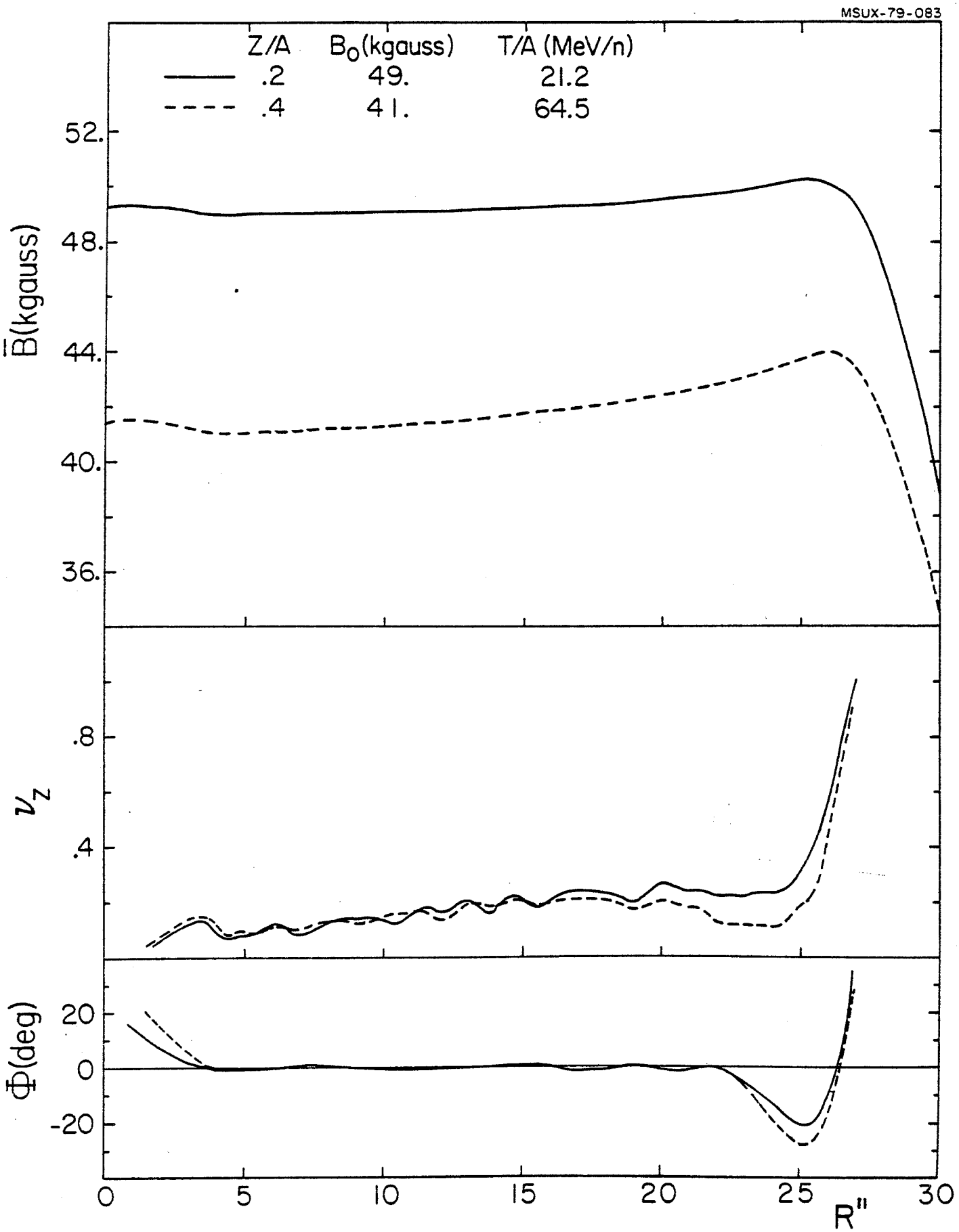

FIG. 22. Average field, ν_z and phase, as a function of the radius, for two ions with Z/A=.2 and Z/A=.4.

radius at which ν_R reaches the same constant value, say ν_R=1 or ν_R=.8 (typical for extraction), shifts inwards in going from the most relativistic beams to the least relativistic ones, a fact which influences the beam extraction. More details on this are given in (6).

In order to analyse the magnetic field in the region where the center plug dominates, the $\bar{B}_{iron}(r)$ fields corresponding to the ions with Z/A=.2, .322, and 0.5, and with B_o values of 49, 45.5, and 36 kgauss respectively, are plotted on an enlarged scale and up to 8" radius in Fig. 23. The cone field is very evident in the region up to 4", with a maximum bump, at the center, of 500-550 gauss.

The total fitted fields, for the same three cases, are shown in Fig. 24. For comparison, the isochronous fields for the same B_o values are plotted as dotted lines. Two features should be noted:

- the cone amplitude does not remain constant at the different excitations, even though the $\bar{B}_{iron}(r)$ very much does. This is due to the combined contributions of the main coils and the trim coils fields which, as shown in Fig. 18, vary both in size and sign. In order to compensate for these unavoidable effects, and have some control in the size of the cone field, a correction coil will be inserted in the plug in the slot existing between the hill part and the cylindrical part (see Fig. 2). The field of such a coil is shown in Fig. 25 for a current of 300 A.

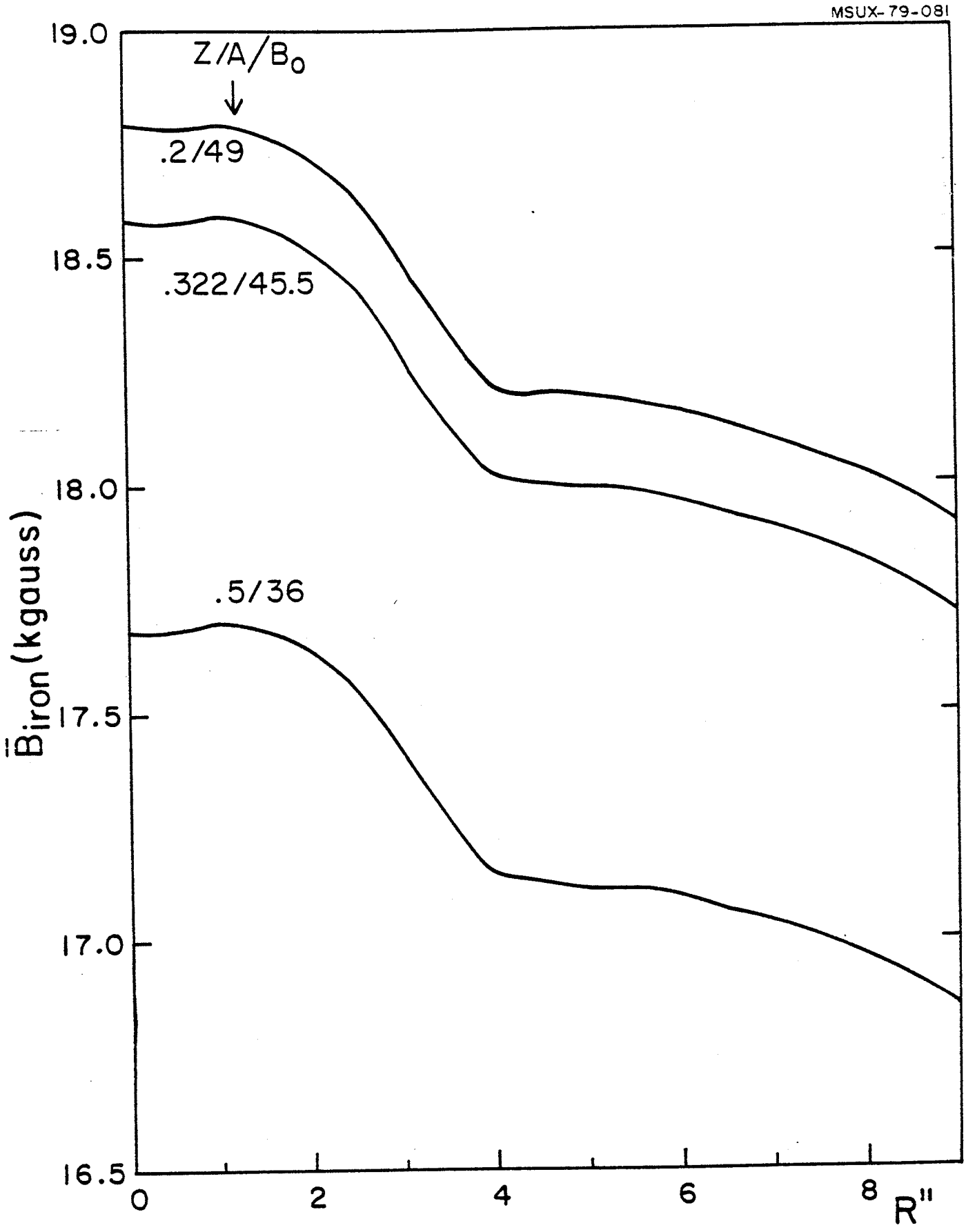

FIG. 23. Iron cone field produced by the plug for different field levels.

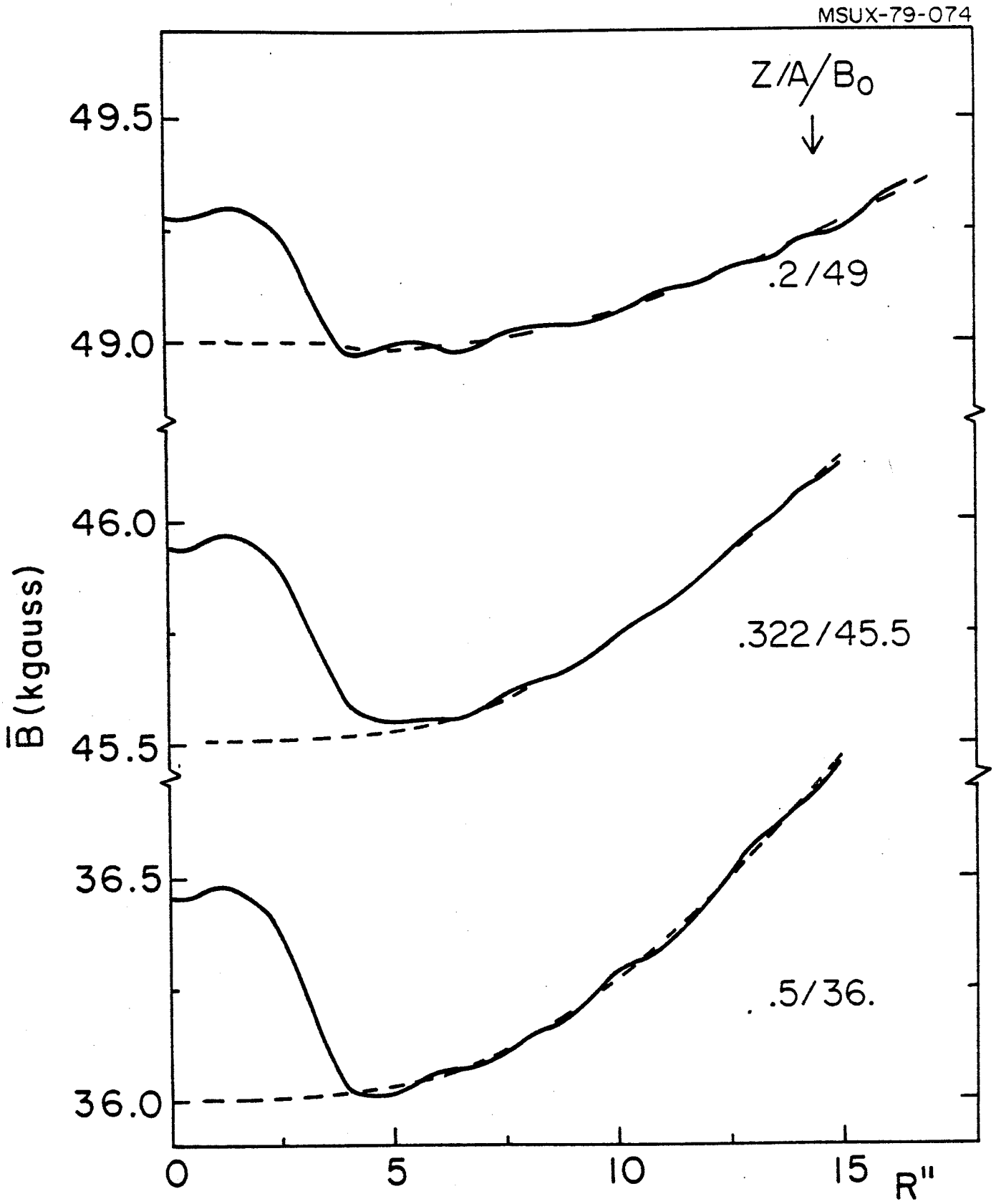

FIG. 24. Total average field for the listed ions. The dashed lines represents the isochronous fields.

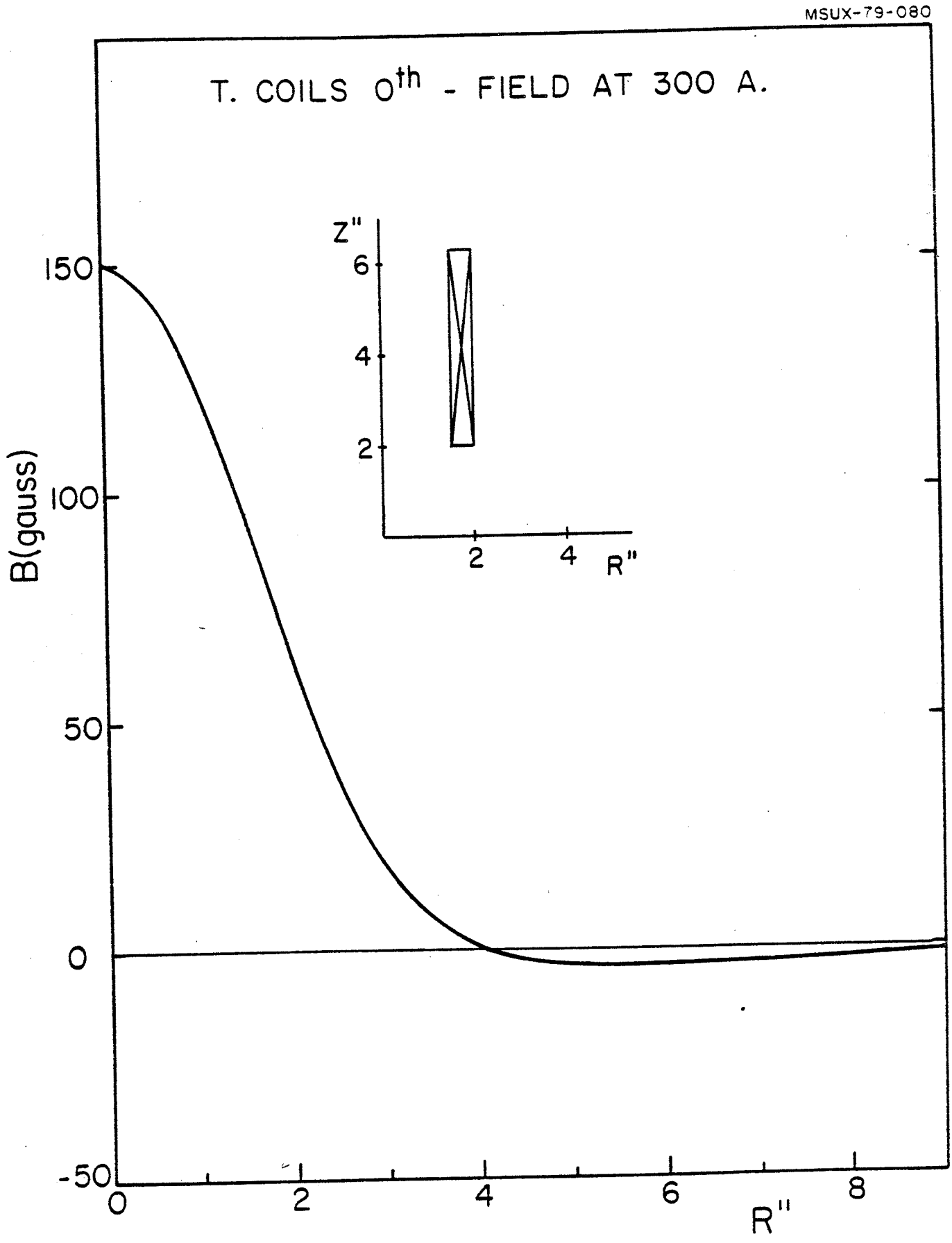

FIG. 25. Air core field produced by the coil 0th (inserted in the plug) at 300 A.

- the enlarged scale of Fig. 24 makes much more apparent the field oscillations around isochronism produced by the trim coils and responsible for the ripples in ν_z.

In order to summarize the focusing properties of the cyclotron, working plots in the (ν_R, ν_z) space are shown in Figs. 26, 27, and 28 for Z/A = .5, .322, and .05 respectively. For each ion the two previously discussed B_o values are presented.

The plots show that in all instances at low fields, the $\nu_R + 2\nu_z = 3$ resonance is rapidly approached at increasingly higher ν_R values. Other resonances, $(\nu_R = 1, \nu_R = 2\nu_z)$, are as in other conventional cyclotrons and should pose no problems in their traversal.

6. Conclusions

Even though this study has focused on the K-500 cyclotron several aspects emerge which have, in our opinion, rather general implications and may therefore be useful for other investigators in this field. We list here the most notable ones:

- it is important to include early in the design all possible details of the pole tip structure (trim coils holes, holes for the R.F. etc.). Their effect on the magnetic field is seldom negligible and may require at later stages, extensive modifications which could result impractical or difficult, because of the freezing meanwhile of other parameters.

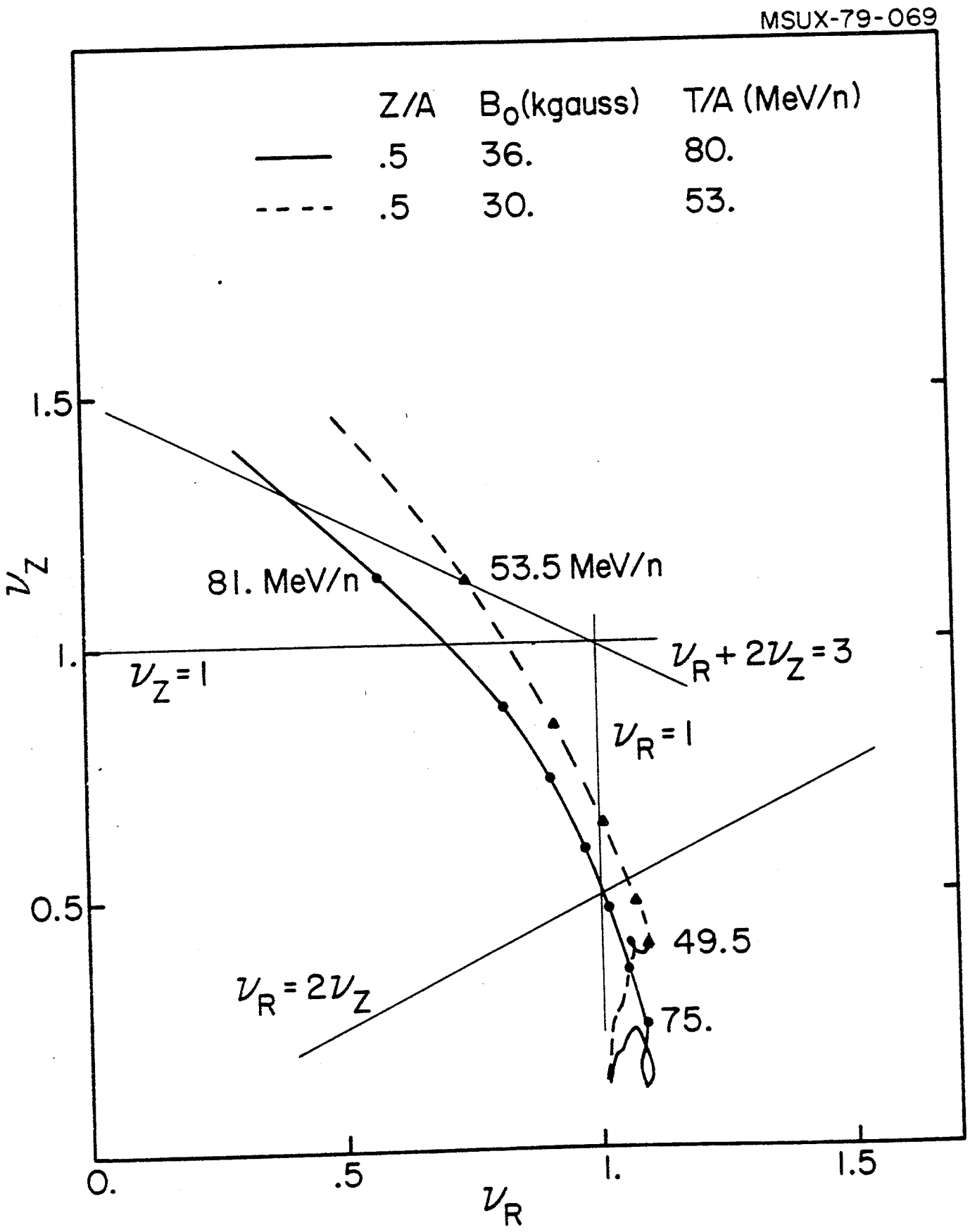

FIG. 26. Operating (ν_R,ν_Z) diagrams for an ion with Z/A=.5 and two different field level.

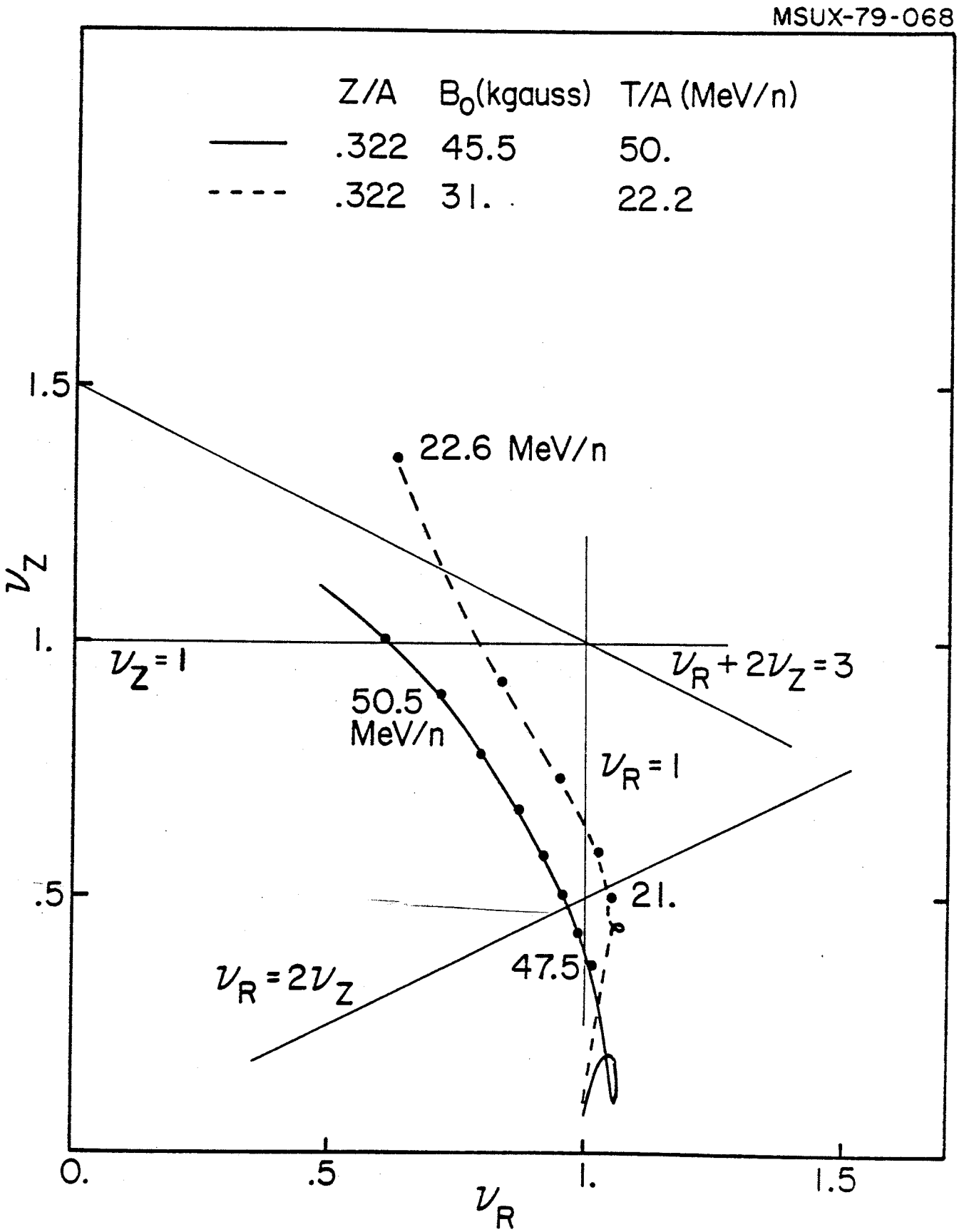

FIG. 27. Operating (ν_R, ν_Z) diagrams for an ion with Z/A=.322 and two different field levels.

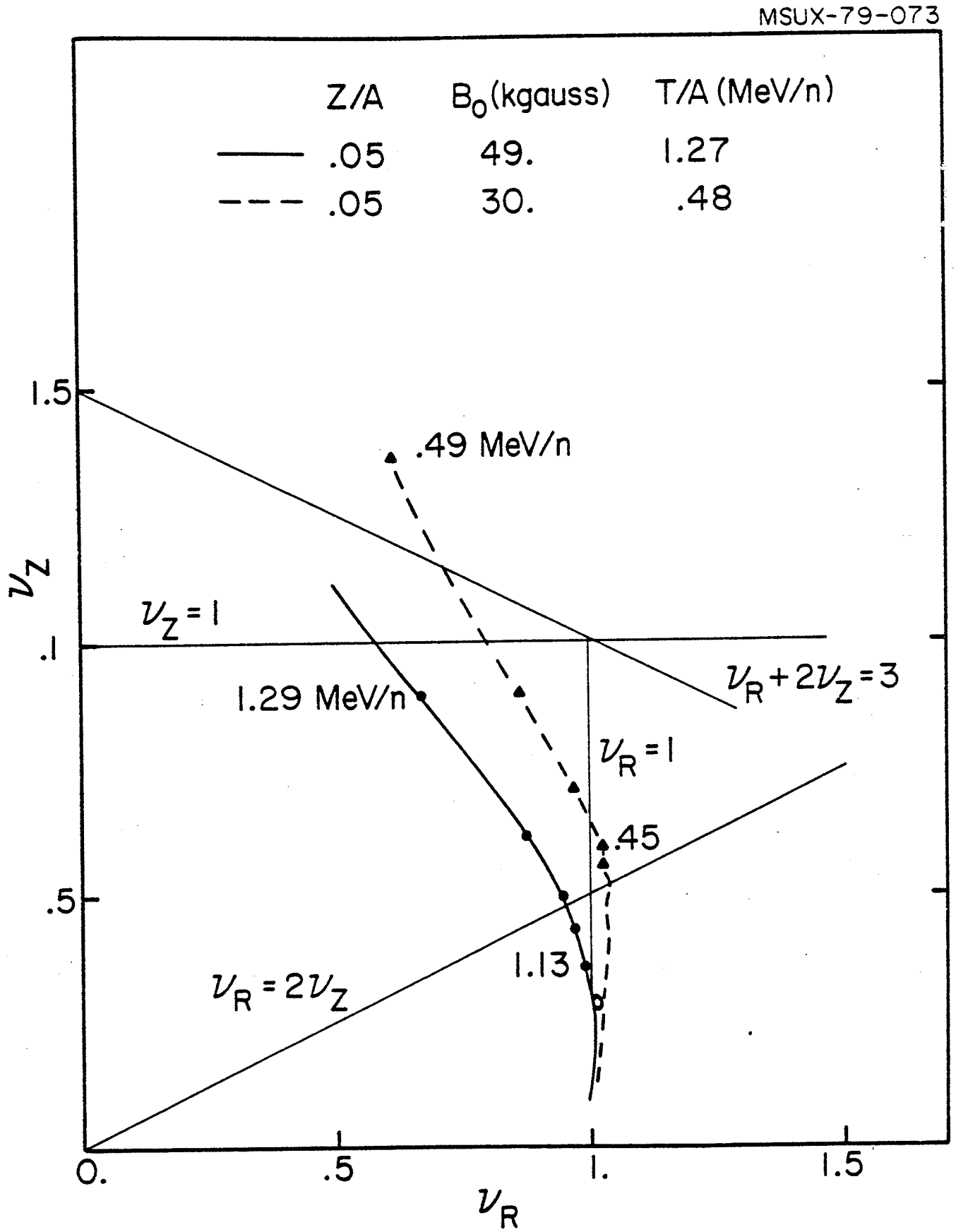

FIG. 28. Operating (ν_R, ν_Z) diagram for an ion with Z/A=.05 and two different field levels.

- the quest for a shape of the iron produced field which minimizes the trim coil power over the machine operating range has not just the estethic goal of decreasing power consumption. In fact it brings the advantage of minimizing the trim coils induced oscillations in the field which, if unchecked, could induce a loss of axial focusing.
- radial shifts in the position of the average field peak should be checked carefully, because of their consequences on the extraction system design. These shifts are unavoidable in any superconducting cyclotron insofar as two-section splitting of the coil is used, which looks now as the only practical solution for achieving isochronism.
- the appearance of unexpected resonances at low fields, caused by the large increase in the flutter, should be investigated.
- if a center cone field is used, which seems a reasonable solution where internal ion sources are planned, the intrinsic lack of control on part of the cone strength implies that some local extra-correction system is needed.

As an overall conclusion for the K-500 cyclotron, this study shows that the desired machine performances can indeed be met, albeit with some modifications of the existing pole geometry. All the modifications described here have been carried out. Final mappings of the field, including the actual measurements of the trim coils field effects are expected to be completed in the next few months.

References

1. H.G. Blosser, The Michigan State University Superconducting Cyclotron Program, IEEE Trans. Nucl. Sci. NS-26 (1979) 2034.
2. G. Bellomo, D.A. Johnson, P. Miller and F.G. Resmini, Magnetic Field Mapping of the K-500 Cyclotron at MSU, to be published.
3. E. Fabrici and F.G. Resmini, Survey of Beam Dynamics prior to Extraction in the K-500 Cyclotron at MSU, to be published.
4. F. Resmini et al., Design Characteristic of the K-800 Superconducting Cyclotron at MSU, IEEE Trans. Nucl. Sci. NS-26 (1979) 2078.
5. E. Liukkonen and T. Antaya, Design of the h=1 Central Region for the K=500 Superconducting Cyclotron, MSU Annual Report 1978-1979, 107.
6. E. Fabrici, D.A. Johnson and F. Resmini, Extraction System for the K-500 Cyclotron at MSU, to be published.